

# On the Impact of Black-box Deployment Strategies for Edge AI on Latency and Model Performance

Jaskirat Singh · Bram Adams · Ahmed E. Hassan

Received: date / Accepted: date

**Abstract** *Context:* Cloud-based black box model deployment faces challenges related to latency and privacy due to data transmission across Wide Area Networks. On the other hand, mobile-based black box deployment prioritizes privacy at the expense of higher latency due to limited computational resources. To address these issues, Edge AI enables the deployment of black box models across mobile, edge, and cloud using a wide range of operators able to distribute a model's components, terminate inference early, or even quantize a model's computations, offering latency and privacy benefits. Deciding what combination of operators to use across the Edge AI tiers to achieve specific latency and model performance requirements is still an open question for MLOps engineers. *Objective:* This study aims to empirically assess the accuracy vs inference time trade-off of different black-box Edge AI deployment strategies, i.e., combinations of deployment operators and deployment tiers. *Method:* In this paper, we conduct inference experiments involving 3 deployment operators (i.e., Partitioning, Quantization, Early Exit), 3 deployment tiers (i.e., Mobile, Edge, Cloud) and their combinations on four widely-used Computer-Vision models to investigate the optimal strategies from the point of view of MLOps developers. *Results:* Our findings suggest that Edge deployment using the hybrid Quantization + Early Exit operator could be preferred over non-hybrid operators (Quantization/Early Exit on Edge, Partition on Mobile-Edge) when faster latency is a concern at medium accuracy loss. However, when minimizing accuracy loss is a concern, MLOps engineers should prefer using only a Quantization operator on edge at a latency reduction or increase, respectively over the Early Exit/Partition (on edge/mobile-edge) and Quantized Early Exit (on edge) operators. In scenarios constrained by Mobile CPU/RAM resources, a preference for Partitioning across mobile and edge tiers is observed over mobile deployment. For models with smaller input data samples (such as FCN), a network-constrained cloud deployment can also be a better alternative than Mobile/Edge deployment and Partitioning strategies. For models with large input data samples (ResNet, ResNext, DUC), an edge tier having higher network/computational capabilities than Cloud/Mobile can be a more viable option than Partitioning and Mobile/Cloud deployment strategies.

**Keywords** Edge AI · Deployment Strategies · Inference Latency · Model Performance

## 1 Introduction

Artificial Intelligence (AI) on the Edge (also "Edge Intelligence" or "Edge AI") [122], an interdisciplinary field derived from Edge computing and AI, is beginning to receive a tremendous amount of interest from

---

Jaskirat Singh  
Queen's University  
E-mail: 21js160@queensu.ca

Bram Adams  
Queen's University  
E-mail: bram.adams@queensu.ca

Ahmed E. Hassan  
Queen's University  
E-mail: hassan@queensu.ca

both the industry and academia. This is primarily because of its high performance, low latency, privacy preservation, and potential independence from network connectivity. Edge AI leverages widespread edge resources instead of relying solely on cloud or mobile, leading to more efficient AI insights for inference and training tasks. For example, in our experiments, we consider inference tasks in a typical Edge AI environment involving an edge device (tier) near a resource-scarce mobile device (tier) and a resource-abundant cloud device (tier) far from the edge device (tier).

Traditional monolithic deployments such as deploying large AI models entirely on a cloud or a mobile tier may affect the overall performance in terms of Key Performance Indicators (KPIs). For example, deploying entire AI models on the cloud may provide faster computation in model inference due to the available GPU resources, however, it may lead to high transmission latency, monetary cost, and privacy leakage when transmitting large amounts of input data across the wide-area network (WAN) to a centralized data center for AI applications (e.g., real-time video analytics). On-device inference running entire AI applications on the mobile tier to process the input data locally does provide data privacy protection, however, it may suffer from high computation latency because many AI applications require high computational power that significantly outweighs the capacity of resource-constrained mobile tiers [97].

Edge computing essentially pushes cloud-like services to network edge servers that are in closer proximity to mobile tiers and data sources [103]. This promises several benefits compared to the traditional cloud-based paradigm (i.e., low transmission latency, data privacy protection, and low monetary cost) and mobile-based paradigm (i.e., faster computational latency). However, this is achieved at the expense of increased computational latency compared to the cloud and a higher data privacy threat compared to the mobile.

Various so-called operators for Edge AI model inference have recently been proposed, most of them treating the model to be deployed as black-box to address the above challenges faced by monolithic mobile, edge, and cloud deployments. Zhou et al. [122] provide a detailed survey on 7 major families of deployment operators. Among the 3 model optimization operator families, Model Compression covers a wide range of operators like Weight pruning, Knowledge Distillation, and Quantization to reduce computation and storage; Model Partition provides computational offloading across the tiers and latency/energy-oriented optimization; and Model Early-Exit performs partial DL model inference at early exit points, basically trading off accuracy for speed. Among the other families, Edge Caching focuses on reusing the previous results of the same inference task for faster response, Input filtering is based on detecting differences between inputs, avoiding redundant computation, Multi-Tenancy supports scheduling multiple DL-based tasks in a resource-efficient manner, and Model Selection uses Input-oriented, accuracy-aware optimization.

Right now, MLOps engineers continuously experiment with different combinations of operators to find an optimal balance in latency and model prediction performance. White-box operators require investing a lot of time in re-training or fine-tuning a model, changing weights and structure, which requires a deep understanding of the internal workings of the model, including its architecture, parameters, and training process. Furthermore, the resulting model may start behaving too unpredictably compared to the model versions tested before. In contrast, the black-box operators allow quicker adaptation to models without the need for an in-depth understanding of their internal architecture or parameters, by applying transformations on pre-trained models. Such operators are often favored in scenarios where model transparency is limited, especially in the case of DNN models.

Given black-box Edge AI operators, the challenge now becomes: 1) Where (on what tiers) to deploy models in an Edge AI setting; 2) How to post-process models using operators to make them compatible with those tiers. The combination of a choice of tier and operator forms an Edge AI deployment strategy. While there are so many deployment operators and tiers, right now MLOps engineers have to do trial and error to find the best configuration. Hence, this study tries to start up a catalog of empirical data to one day have recommendation systems to assist the MLOps Engineers of a given company in deciding which deployment strategy is the most appropriate for their context.

The main contribution of this study is an in-depth empirical comparison between competing Edge AI deployment strategies to suggest recommendations for the deployment of DNN models for MLOps engineers. In particular, we compare strategies mapping 3 common black-box deployment operators (i.e., Partitioning, Early Exit, Quantization) and their combinations (Quantize Early Exit and Quantize Early Exit Partition) to 3 common deployment tiers (i.e., Mobile, Edge, Cloud) and their combinations in an Edge AI Environment. Second, for each of the Edge AI deployment strategies, this study evaluates the

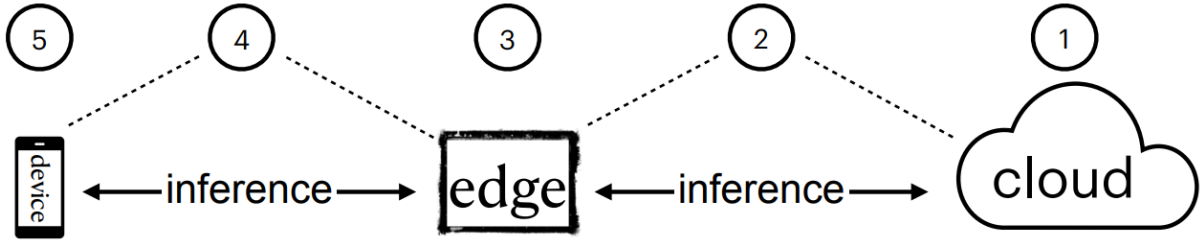


Fig. 1: Graphical overview of Single-tier (1,3,5) and Multi-tier (2,4) Edge AI Deployment Strategies

end-to-end (round trip) latency in an Edge AI setup (MEC tiers). The third contribution is our focus on measuring the latency of deployment strategies across a wide range of varying input (i.e., images) sizes using sequential inference requests. Our study analyzes the optimal trade-off in terms of inference latency and accuracy among competing Edge AI deployment strategies. We address the following research questions:

- RQ1: What is the performance impact of single-tier deployment in an Edge AI Environment?
- RQ2: What is the performance impact of the Quantization operator within and across the tiers of the Edge AI Environment?
- RQ3: What is the performance impact of the Early Exiting operator within and across the tiers of the Edge AI Environment?
- RQ4: What is the performance impact of the Model Partitioning operator across the tiers of the Edge AI Environment?
- RQ5: What is the performance impact of Hybrid operators within and across the tiers of the Edge AI Environment?

Answering the research questions formulated above will guide MLOps engineers and researchers in the AI field to better understand and assess the impact of how and where black-box models are deployed in an Edge AI Environment. The results of this paper are valuable for MLOps engineers who are debating on what would be the most feasible choice for performing inferences in the context of Edge AI.

The rest of this paper is structured as follows. Section 2 talks about the Background of the study. Section 3 presents prior works in this field. Section 4 explains approach details including Subjects, Experimental Setup, Metrics for evaluating model performance, Motivation and Approach for each research question, and Data Analysis. Section 5 describes the results for the five research questions. Section 6 discusses the results and compares the results of the RQs. Section 7 proposes the threats to the validity of the paper which is followed by the conclusion in Section 8.

## 2 Background

### 2.1 Deep Learning Architecture

The architecture of a Deep Learning (DL) model is composed of layers that transform the input data using mathematical operations to produce an output. Layers are organized sequentially to form a Deep Neural Network (DNN) architecture [49]. The resulting computational graph represents the flow of data and computations through a neural network, i.e., a representation of how the layers are connected and how data moves from one layer to another. Each layer is a node in the graph, and the connections between nodes (edges) show the data flow. A node encapsulates the entire computation performed by that layer, including all its individual elements. However, the individual elements within a layer, such as neurons, weights, biases, activation functions, and other internal components, are not explicitly represented as separate nodes in the graph. This graph structure allows frameworks to efficiently execute forward and backward passes (propagation) during training and inference processes.

During the training process, the forward pass computes predictions and loss, while the backward pass computes gradients for weight updates to minimize the loss. During the inference process, only the forward pass is used to make predictions or generate output based on input data. Weights are the learnable parameters associated with the layers in the model. These parameters are learned during

training to optimize the model’s performance. Activations are the intermediate outputs produced by layers as data flows through the computational graph [1].

## 2.2 Monolithic Edge AI Deployment

The traditional deployment of an entire model on mobile or cloud (tiers 1 and 5 in Figure 1) for inference has some important limitations. For example, deploying the entire AI model on a mobile device leads to slower computation whereas on the cloud it leads to higher transmission latency and potential data privacy threats. Various researchers have experimented with ways to deploy models on the edge device (like 3 in Figure 1) due to its closer proximity to the mobile device and faster computational capabilities than a mobile device [32, 58]. However, edge devices are often smaller and less powerful than centralized servers or cloud resources, which limits their processing power. To address these limitations, there is a need for alternative deployment strategies (i.e., Model Partitioning, Model Compression, Model Early Exiting) that aim to mitigate these challenges.

## 2.3 Multi-tier Edge AI Partitioning

The Multi-tier Edge AI deployment Strategy (e.g., tiers 2 and 4 shown in Figure 1) partitions (splits) an AI model between Edge-Cloud and Edge-Mobile tiers, respectively. This can overcome the limitations of traditional deployment strategies by enhancing data privacy, increasing computation efficiency, reducing memory requirements, improving scalability, and providing a flexible architecture that can be easily adapted to different use cases and deployment scenarios.

The key insight is the observation that most of the strategies used to enable partitioned model inference across, for example, mobile and edge devices, operate on the computation graph underlying modern deep learning architectures [28]. Such graphs express the different elements of neural networks, as well as the calculations performed while traversing edges in the graph. By finding the right edges to split, one can implement model partitioning, effectively obtaining two or more sub-graphs.

Overall, model partitioning is a powerful strategy for optimizing the deployment of deep neural network models on resource-constrained devices. This family of Edge AI operators can partition models across the tiers of an Edge AI Environment:

- Mobile-Edge Partition: The mobile device receives the input data, performs inference on the first half of the model, and then sends the intermediate output to the edge device. Afterward, the edge device performs inference on the second half of the model using the received intermediate output from the mobile device. Finally, the edge device sends the final output back to the mobile device.
- Mobile-Cloud Partition: The mobile device receives the input data, performs inference on the first half of the model and sends the intermediate output to the cloud device via the edge device. Then, the cloud device performs inference on the second half of the model using the received intermediate output from the edge device. Finally, the cloud device sends the final output back to the mobile device via the edge device.
- Edge-Cloud Partition: The mobile device first receives the input data and sends it to the edge device as it is. Then, the edge device performs inference on the first half of the model using the received input data and sends the intermediate output to the cloud device. The Cloud device further performs inference on the second half of the model using the received intermediate output from the edge device. Finally, the cloud device sends the final output back to the edge device, which in turn sends it back to the mobile device.

## 2.4 Early Exiting

Early Exiting is another family of Edge AI deployment operators allowing DL models to exit a model’s computation process early rather than waiting for the full forward pass to complete [91]. The basic idea is to introduce an early exit point at a particular layer of the neural network, allowing the model to make predictions based on the intermediate output without completing the full forward pass.

The benefits of model early exiting include faster inference speed, reduced energy consumption, and increased model efficiency at the cost of lower accuracy performance. Implementing early exiting on a trained model can help improve the model’s runtime performance, especially if the model was initially designed for high accuracy and not optimized for efficiency.

## 2.5 Quantization

Quantization [31] is a member of the Model Compression family of Edge AI deployment operators, where the neural network’s calculation is reduced from full precision (i.e., 32-bit floating point format) to reduced precision (e.g., 16-bit, 8-bit integer point format) to decrease both the computational cost and memory footprint, which makes inference more scalable on resource-restricted devices [46].

Post-training quantization (PTQ) and Quantization-aware training (QAT) [27] are common techniques used in machine learning to optimize deep neural networks for deployment on hardware with limited numerical precision, such as CPUs, GPUs, and custom accelerators. PTQ involves applying quantization to the weights and activations of a pre-trained model after it has been trained to reduce the memory footprint and computation requirements of the model. This can be done using techniques such as static or dynamic PTQ. In dynamic PTQ, the quantization parameters are dynamically calculated for the weights and activations of a model during run-time and are specific for each inference, while, for static quantization, the quantization parameters are pre-calculated using a calibration data set and are static during each inference.

QAT on the other hand involves incorporating quantization into the training process itself. This can be done using techniques such as fake quantization or simulated quantization, which simulate the effects of quantization on the weights and activations during the forward and backward passes of training. By training the model to be more robust to quantization, QAT can result in models that are more accurate after quantization than PTQ. QAT typically involves two stages: calibration, where the appropriate range of values for the weights and activations is determined, and fine-tuning, where the model is trained with the quantized weights and activations.

## 2.6 ONNX Run-time for Inference

ONNX (Open Neural Network Exchange)<sup>1</sup> is a standard format built to represent inter-operable AI models that can run on a variety of hardware platforms and devices. The core of the ONNX model is the computational graph, which represents the structure and computations of the model. The computational graph consists of nodes that represent individual operations or layers in the model. The nodes take input tensor(s), perform the specified operation, and produce output tensor(s). The nodes have attributes that define the type of operation, input and output tensors, and any parameters or weights associated with the operation.

The ONNX Runtime<sup>2</sup> is a high-performance Inference Engine for deploying ONNX models to production for real-time AI applications. It is optimized for deployment on various devices (i.e., Mobile, Edge, and Cloud) and hardware platforms (i.e., CPUs, GPUs, and specialized accelerators). We consider ONNX as the subject models’ format and the ONNX Run-time as an Inference Engine for this study.

ONNX Runtime Execution Providers are a set of plug-ins that enable the execution of ONNX models on a wide range of hardware and software platforms. The ONNX Run-time supported Execution Providers that we studied and considered as a back-end for hardware acceleration while performing model inference are the CUDA Execution Provider, which uses GPU for computations, and the default CPU Execution Provider, which uses CPU cores for computation.

## 3 Related Work

In previous surveys [122, 103, 14, 75], 8 families of Edge AI model inference operators are discussed: Model Compression (Quantization, Weight Pruning, Knowledge Distillation), Model Partition, Model Early-Exit, Edge Caching, Input Filter, and Model Selection. Moreover, Matsubara et al. [68] conducted a

---

<sup>1</sup> <https://onnx.ai/>

<sup>2</sup> <https://github.com/microsoft/onnxruntime>

Table 1: Distinctive Features: Prior Work vs. Our Approaches

<sup>1</sup> P: Partitioning, Q: Quantization, E: Early Exiting, X: Quantize Early Exit, V: Quantize Early Exit Partition, L: Combination of Partitioning and Quantization, I: Combination of Partitioning and Early Exit, OO: Other Operators (BI: Bottleneck Injection, PR: Pruning, KD: Knowledge Distillation), BT: Black-Box Transformations, SS: Simulated Setup (empty cell represents Real or Emulated Hardware Setup), M: Mobile, E: Edge, C: Cloud, ILA: Inference Latency Approach (S: Sequential, A: Asynchronous, NM: Not Mentioned), ID: Image Data, TD: Textual Data, RoI: Range of Input Sizes (for latency evaluation), AoA: Analysis of Accuracy, CaO: Comparison across Operators, Empty cells of MEC mean they are not an Edge AI setup

comprehensive survey of the various approaches for Partitioning, Early Exiting, and their combinations with each other and with other operators (such as Bottleneck Injection, Pruning, and/or Knowledge distillation). As summarized in Table 1, many studies focus on in-depth analysis of individual operators or comparing two different operators. Only one study [67] considers three operators, suggesting that there is limited research comparing a larger set of operators within the context of Edge AI. Evaluating three (or more) operators allows for a more comprehensive analysis of their relative performances and trade-offs, which is a focus point of our study.

Among the various kinds of operators, we focus on operators that correspond to model transformations, i.e., modifications in the structure, parameters, or behavior of ML models. This subset of operators can be further categorized into white-box and black-box operators. In previous studies, the white-box operators discussed are Model Pruning and Knowledge Distillation, and the black-box operator discussed is Model Partitioning. Some of the operators like Model Quantization, Model Early Exiting, and Bottleneck Injection can be performed in both black box and white box manner. In real-world scenarios, applying white-box operators to ML models requires thorough domain expertise about their internal workings to

fine-tune or retrain them, due to which there is a practical need to focus on black-box operators that can optimize models without fine-tuning or retraining. Therefore, we narrowed down our study to the black-box operators (i.e., Model Partition, Model Early Exit, Model Quantization) and their combinations to provide empirical data aimed at understanding how to optimize models robustly and tackle the challenges posed when deploying to heterogeneous Edge AI environments. Among the black box operators, we excluded the Bottleneck Injection operator as it focuses on intermediate data compression techniques (such as lossless/lossy compression, clipping, etc) and does not inherently perform transformations on the DNN models themselves, which is the goal of our study.

Table 1 compares the distinctive features of our study and previous studies. Among the 10 studies focusing on non-hybrid Partitioning operator, all of them were performed by black-box transformations, which suggests that this operator requires no retraining or fine-tuning. Among the 25 Early Exit studies, 2 studies were performed in a black box manner, which shows that it is feasible to perform Early Exiting without retraining or fine-tuning. Among 21 Quantization studies, the majority of them (16) were performed in a black-box manner, indicating that this approach is more commonly used. In terms of hardware setup, 4 of the previous studies consider simulated setup, indicating that it is feasible to consider this kind of setup for testing the operator’s performance. In terms of MEC tiers, only 2 studies consider all 3 MEC tiers, suggesting that this area of research is relatively less explored. In terms of MEC tiers, Inference Latency Approach, and Range of Inputs, no study considers sequential inference of a range of inputs (with varying sizes) in an Edge AI setup (MEC tiers), which was explored in our study. In terms of input data, the majority of studies (64) consider image data, indicating that this type of data is more commonly used for the mentioned operators.

In Table 1, there are limited studies (only 2) that consider all three tiers (i.e., Mobile, Edge, Cloud) for Edge AI setup in their experiments. Considering all three tiers collectively provides a more holistic view of real-world deployment scenarios with varying computational and network conditions. Therefore, we considered all three tiers to ensure a comprehensive and versatile approach in our Edge AI setup. Four prior studies [113, 76, 16, 74] employ a simulated Edge AI Setup instead of real hardware, the former is more cost-effective and more accessible than real hardware, while also providing a controlled environment, making it easier to isolate and micro-benchmark the latency performance of individual operators. On the other hand, while simulations can closely approximate the behavior of real hardware, they may not replicate all the nuances and complexities of a real-world environment such as hardware/network variability, power consumption, and real-time constraints.

Among the studies considering interconnected multi-tier networks, the majority (20) consider Sequential Inference in comparison to Asynchronous Inference (i.e., 9) for latency evaluation across the tiers. In sequential inference, the inference tasks proceed in a step-by-step manner across the tiers of the network and are dependent on each other (i.e., the next inference task waits for the completion of the previous inference task). In asynchronous inference, the inference tasks across the tiers are performed concurrently or independently from each other. We considered Sequential inference as it allows us to isolate the performance characteristics of individual operators in a controlled environment. In other words, it allows for uncovering a more deterministic impact of input data sizes and network/computational resources of heterogeneous MEC tiers on the operators’s latency performance, similar to how micro-benchmarks operate.

The majority of the prior studies focus on image data instead of textual or speech data as input for inference of these black box operators due to its prevalence in real-time deployment scenarios. Image data is often more complex and less interpretable than text or speech data, requiring more bandwidth for transmission and more storage space than text or speech data typically due to its larger size. It requires more computational resources to process possibly due to their usage in computationally intensive tasks like object detection, image classification, and image segmentation. As a result, this is why Computer Vision models are commonly studied in prior work, requiring image data as input for inference. As such, we narrowed down the scope of the data and model in our study to the CV domain.

To conclude, our paper provides a novel empirical study of Edge AI Deployment Strategies, which are mappings of the black-box operators (i.e., Partition, Early Exit, Quantization), and their combinations, onto Edge AI tiers (i.e., Mobile, Edge, Cloud), and their combinations, to analyze the optimal trade-off in terms of latency and accuracy in real-time deployment scenarios. The previous studies, as mentioned in Table 1, combine Partitioning with either the Early Exit [76, 100, 116, 48, 67] or Quantization operator [53]. In our study, we went one step further and analyzed unexplored combinations among these three operators, like Quantization + Early Exit and Quantization + Early Exit + Partition. To our

knowledge, there is no comprehensive study in previous work (Table 1) on the comparative analysis of these three black-box operators and their specific combinations in the context of Edge AI to decide which operator is optimal in which deployment scenario. Secondly, our study in comparison to previous studies (Table 1), evaluates the end-to-end (round trip) latency of the deployment strategies in an Edge AI setup (MEC tiers). The third contribution is our focus on measuring the latency of deployment strategies across a wide range of varying input (i.e., image) sizes using sequential inference requests (which have not been explored in previous studies). This contribution helps in analyzing the impact of input data on the proposed deployment strategies.

Below, we discuss existing work related to the 3 operator families which we considered in our study.

### 3.1 Partitioning

The Model Partitioning operator performs black-box transformations splitting a given model into head (1st half partition) and tail (2nd half partition) sub-models at a partition point such that the two sub-models, when feeding the output of the head into the input of the tail, produces the same output as the original model. While in some studies [7,11], the partitioning point is chosen heuristically, in the majority of studies performing Model Partitioning ([20,43,45,53,116,82,16,113,74,56,39]), various factors like computational load, network cost, energy consumption, input data sizes and/or privacy risk are evaluated for each of the partitioning points of the DNN models during deployment across the Edge AI environment to inform the selection. There is no generalized optimal partition point, as it varies for models with different architectures [68]. Therefore, in our study, we simplified our approach by considering equal-size (MB) partitioning to do a fair evaluation of each of the subjects considered in our study.

Many of the CV models (i.e., AlexNet, VGG 11/16/19, DenseNet, ViT, NiN, ResNet 18/34/50/56, GoogLeNet, AgeNet, GenderNet, Inception-v3, BNNs, eBNNs) considered in previous studies [113,16, 74,45,56,39,43,82,53,120,7,20,100,116,48] for model partitioning based on black box transformations have weak accuracy performance and model complexity within reach of resource-constrained mobile tiers. However, in our study, more accurate and complex state-of-the-art CV models are considered (such as Wide ResNet-101, ResNext-101, FCN, and DUC) to analyze the latency vs accuracy trade-off in an Edge AI environment with heterogeneous MEC tiers.

The Bottleneck Injection (BI) operators have also been previously studied in combination with Model Partitioning to reduce the transmission, computation, and energy costs across the MEC tiers. These introduce artificial bottlenecks to DNN models by compressing the intermediate data, modifying the DNN architecture, and/or both. The Bottleneck Injection techniques that do not involve re-training of DNN models include Intermediate Data Compression using Quantization, Tiling, Clipping, Binarization, Entropy Coding, and Lossy/Lossless Compression, which are analyzed in a few previous studies [7,20, 11]. However, most of the BI operators require extensive re-training of models as they Modify the DNN architectures with Auto Encoders [21,40,8,92,50,42,114,3,90,65,69,70], Head Network Pruning [42], and Head Network Distillation [64,66,67,3,90,65,69,70]. The mentioned black-box and white-box BI operators may affect the accuracy performance due to intermediate data compression and architectural modifications, respectively.

In our study, we treat the partitioning operator as a black box transformation of a model into two sub-models (this number is commonly used in previous studies) that do not modify the input or intermediate representations in the models (i.e., the final output will not change), hence, preserving the accuracy. This is important, because the Bottleneck Injection operators can be costly and time-consuming (especially the ones involving architectural modifications), and would change the known, possibly certified behavior of an existing model.

### 3.2 Early Exiting

The core idea of Early Exiting is to enable a DNN model to make early predictions without having to wait until the entire computation process is completed by terminating the execution at early exits/classifiers/subbranches. In the majority of the previous studies, the early exits require re-training of the base models either by joint training or separate training. In Joint training, the (early) exits are trained simultaneously with a model [19,48,60,84,95,99,100,101,104,109,111,112,116,121] by defining

a loss function for each of the classifiers and minimizing the weighted sum of cross-entropy losses per sample. In contrast, in separate training [59, 67, 110, 106], model training is performed in the first stage then the training of the early exits is performed, such that the pre-trained model parameters are frozen. There are some studies [29, 30] that perform Early Exiting by comparing the output of an early exit with the corresponding class means using Euclidean distance. If the output of an early exit is not close enough to a class mean, the execution continues and the same process is performed for the next early exit in the DNN model. In other words, the early exiting is performed dynamically at inference in a black box manner.

In our study, we achieve a similar effect of early exiting by performing manual and static modifications on the computational graphs of the subject models to short-circuit (skip) the similarly structured graph computations. The motivation behind this approach lies in the flexibility and customization it offers in the ONNX framework to MLOps Engineers.

### 3.3 Quantization

As explained in previous literature surveys [27, 107], there are two popular quantization approaches used to reduce the numerical precision of model parameters, i.e., Quantization-Aware Training (QAT), and Post-Training Quantization (PTQ).

Quantization Aware Training (QAT) involves simulating quantization effects during the training process [22, 93, 89, 98, 35]. In particular, the standard forward/backward passes are executed on a model that uses floating-point precision, and the model parameters are quantized after each gradient update. The QAT quantization method needs training data and back-propagation for its fine-tuning process, which requires a full training pipeline, takes significant extra training time, and can be computationally intensive when dealing with large and complex neural networks.

An alternative to the more resource-intensive Quantization-Aware Training (QAT) method is Post-Training Quantization (PTQ). PTQ involves the quantization of weights and activations along with adjustments to these quantized values, all without the need for fine-tuning (i.e., in a black box manner) [4, 5, 9, 23, 25, 36, 51, 71, 77, 94, 26, 41, 119, 55]. The advantage of PTQ lies in its low and often negligible overhead. Unlike QAT, which relies on a substantial amount of labeled training data for retraining, PTQ is advantageous in scenarios where data is limited or unlabeled. Moreover, we observed that 16 studies considered the black box quantization (Post-Training Quantization) and only 5 studies focused on white box quantization (Quantization-aware training) as shown in Table 1. This suggests that black box quantization is more common and is therefore considered for evaluation in our study. We keep the pipeline more straightforward by performing Static PTQ quantization, which just requires representative data (i.e., validation set in our study) to compute statistics such as mean and standard deviation of weights and activations.

## 4 Approach

This section details the approach followed to address the RQs outlined in the introduction.

### 4.1 Subjects

A set of four pre-trained, state-of-the-art models from the ONNX Model Zoo <sup>3</sup> and Pytorch Imagenet Models store<sup>4</sup> is used as a suitable and representative sample of subjects for the experiment. In this study, we focus on computer-vision tasks as they often demand significant computational and network bandwidth resources during deployment in real-world scenarios. To support the generality of the results, we ensure that the models are heterogeneous in terms of architecture, size, scope, and data set. Furthermore, to obtain findings on realistic models, we selected 4 large and complex image classification and segmentation models, as shown in Table 2.

---

<sup>3</sup> <https://github.com/onnx/models>

<sup>4</sup> <https://pytorch.org/vision/main/models.html>

Image classification is a type of machine learning task where the goal is to assign a label or category to an input image. This is achieved by training a model on a dataset of labeled images, then using that model to predict the labels of new, unseen images [62]. Image segmentation is the process of dividing an image into multiple segments or regions. The goal of image segmentation is to simplify and/or change the representation of an image into something more meaningful and easier to analyze. The output of image segmentation is a set of segments that collectively cover the entire image or a set of contours extracted from the image [73].

The ILSVRC (ImageNet Large Scale Visual Recognition Challenge) dataset is used for evaluating the performance metrics of both the ResNet and ResNext subjects as it is widely used for training and evaluating image classification models. As the network architecture of the ResNet and ResNext subjects is similar, we used different versions of pre-trained weights for ResNet (i.e., IMAGENET1K\_V2) and ResNext (i.e., IMAGENET1K\_V1) from the torchvision package to obtain a better generalization of our results. We used the COCO (Common Objects in Context) and Cityscapes datasets for evaluating the performance metrics of the FCN and DUC subjects, respectively. For the Image Classification subjects, we exported the ResNet and ResNext models from the torchvision.models subpackage to ONNX using the torch.onnx.export() function. For the Image Segmentation subjects, we used the models from ONNX Model Zoo.

Table 2: Subjects of the experiment

Model Name	Model Size	Parameters	Scope	Dataset
ResNet [115]	484MB	126.81M	Image Classification	ILSVRC 2012 [88]
ResNext [108]	319MB	83.35M	Image Classification	ILSVRC 2012 [88]
FCN [61]	199MB	51.89M	Image Segmentation	COCO 2017 [57]
DUC [102]	249MB	65.14M	Image Segmentation	CityScapes [13]

## 4.2 Study Design

From the overall set of 8 operator families for Edge AI Inference discussed in Section 1, we narrow down the scope of our study to delve deeper into strategies that can optimize models in a black box manner for deployment on resource-constrained and network-constrained Edge AI deployment scenarios. In other words, the operators transform the models as-is instead of fine-tuning models (which would invalidate prior model validation results). Among the model optimization operators, we selected 3 operators based on their representativeness (i.e., capable of addressing different aspects of model optimization, such as improving inference speed, providing better data privacy, optimizing resource usage, and reducing model size) and feasibility (i.e., the implementability of operators in black box models).

Eventually, we selected one representative operator (i.e., Quantization) out of the 3 Model Compression operators (i.e., Quantization, Weight Pruning, Knowledge Distillation) as they all focus on a common goal of reducing the size and complexity of black-box models while preserving their accuracy as much as possible. Using the Quantization operator in the ONNX Runtime framework offered by the Intel Neural Compressor tool, quantization can be performed by using the 3 widely used techniques discussed earlier, i.e., Static PTQ, Dynamic PTQ, and QAT. In our study, we used Static PTQ as Dynamic PTQ requires higher computational overhead during inference compared to static PTQ. QAT was excluded from the selection as it involved re-training models, while we focused on post-processing black-box models.

Model Partitioning was selected as it provides computational load splitting across the tiers (i.e., mobile, edge, and cloud) of an Edge AI environment during distributed inference, enabling more efficient utilization of resources and providing scalable deployment of models. It also aims to provide better data privacy than the monolithic edge and cloud deployments by transmitting intermediate outputs rather than the raw input data across the tiers of the Edge AI Environment.

The motivation for considering Early Exiting as an operator is its aim to save computational resources and reduce the time required to predict by exiting early during the forward pass of the neural network.

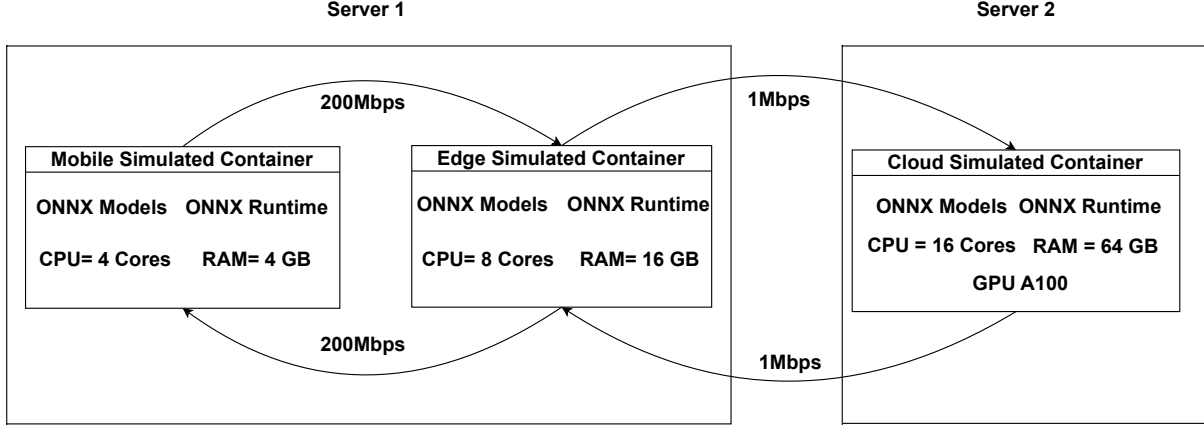


Fig. 2: Graphical illustration of Experimental Architecture for Edge AI

This would especially be valuable in scenarios where resources are constrained (i.e., mobile and edge tiers).

These 3 operators and their combinations are configured on black-box models for inference, depending on where the transformed (fragments of) black-box models will reside among the 3 tiers of the Edge AI Environment. This strategic configuration is vital for achieving optimal performance, minimizing latency, and improving the scalability of Edge AI Deployment. By aligning these operators with the unique characteristics and constraints of each tier, a more effective and adaptable Edge AI ecosystem can be developed, catering to a wide range of use cases and scenarios.

In our study, we perform manual modifications of black-box models to obtain partitioning of original models, early exiting on original/quantized models, and partitioning of quantized early exit models. By executing these modified models in various deployment scenarios, across mobile, edge, and cloud tiers, we then collect empirical data to analyze how each operator, and their combinations, perform under real-world conditions.

In particular, we analyze the trade-off between two quantitative metrics, i.e., inference latency and inference accuracy. This analysis plays a crucial role in understanding the dynamic interplay between performance and latency within the Edge AI Environment, guiding the selection of optimal strategies based on a deployment engineer's use cases and requirements. Some use cases might prioritize low latency at the expense of accuracy, while others could emphasize accuracy even if it leads to slightly higher latency. The empirical data collected from deploying various operators on different tiers provides a quantitative basis for evaluating this trade-off and serves as a foundation for our long-term objective (outside the scope of this paper): the creation of recommendation systems to automatically suggest the most appropriate operators and deployment strategies for specific use cases, aligning with desired latency and accuracy requirements.

### 4.3 Experimental Setup

We simulated an Edge AI deployment architecture for mobile, edge, and cloud tiers interconnected with each other as illustrated in Figure 2. This architecture is designed to support AI inference tasks in both a monolithic and distributed manner for various deployment operators. Based on previous studies [86, 85], we used docker containers to simulate the hardware configurations of actual mobile, edge, and cloud tiers. Docker is an open-source containerization technology ensuring a consistent and easily portable environment (or container) [72]. A container is a lightweight and portable package that includes all the necessary dependencies, libraries, and configurations to run a software application. Docker provides a way to package and distribute applications in a standardized and portable format that can run on any platform, including cloud, on-premise, and edge.

To address the heterogeneous nature of the resource-constrained mobile and edge tiers, we deploy the ONNX Run-time executor with the CPU Execution Provider of the mobile and edge tiers on one server using resource-conscious docker containers. The docker containers simulating mobile and edge tiers

were configured with quad-core and octa-core CPUs (Intel(R) Xeon(R) E7-4870 2.40GHz) along with 4GB RAM and 16GB RAM, respectively, these configurations are based on previous studies [17, 15]. We considered CPU-based edge simulation to represent real-world scenarios where edge devices often do not have dedicated GPUs due to power, size, or cost constraints. The docker container simulating the cloud was configured on a different server than the simulated mobile and edge containers. The simulated cloud container contains 16-core CPUs (Intel(R) Xeon(R) Platinum 8268 CPU 2.90GHz), 64GB RAM, and an NVIDIA A100 GPU, these configurations are based on previous studies [47, 87]. The cloud runs all inference experiments on its GPU using ONNX Run-time with CUDA Execution Provider.

For the 3 simulated docker containers, we use the python:3.9-slim image as a base, on top of which we installed the necessary Python packages including a replica of the ONNX Run-time configuration (the out-of-the-box installation of the ONNX Run-time Python package). Here, the simulated mobile/edge/cloud device is a virtual representation of a physical mobile/edge/cloud device created and operated within a software-based simulation environment (i.e., docker). The docker simulations provide a flexible and convenient way to configure and customize virtual environments that mimic various hardware specifications, network conditions, and software configurations of real-time deployment scenarios. Moreover, the advantages of cost-effectiveness and controlled testing make docker simulations an invaluable tool for conducting inference experiments.

The simulated mobile and edge containers are interconnected to a common network bridge in docker to exchange API requests with each other. The edge container further connects with the external, simulated cloud container. We configured the Linux Traffic Control utility<sup>5</sup> inside each configured docker container for simulating mobile-edge and edge-cloud network bandwidths. After applying a given combination of operators, we placed the resulting .onnx files for the subject models on the corresponding simulated devices. The Flask Framework handles incoming and outgoing requests across mobile, edge, and cloud devices. Base64 encoding is used while transferring data across the devices as it allows the data to be transmitted in a more reliable and universally readable format. For ResNet/ResNext and FCN/DUC models, the final output that is transmitted across the Edge AI Environment is the predicted label or the segmented image, respectively, which both have smaller sizes than the network bandwidths of the Edge AI Environment.

Similar to earlier work, [78, 118, 96, 24, 2], an edge-cloud bandwidth of 1 Mbps was used for simulating the WAN (Wide Area Network) transmission latency, and the mobile-edge bandwidth of 200 Mbps was used for simulating the WLAN (Wireless Local Area Network) transmission latency. The selected bandwidth values aim to represent typical network conditions found in WAN and WLAN environments. WAN connections are prevalent for communicating between edge and cloud over large geographical distances and often have lower bandwidth due to factors like network congestion and long-distance transmission. On the other hand, WLAN connections commonly used for mobile and edge devices placed in closer proximity to each other, tend to provide higher bandwidth.

The entire validation set for running inference experiments is computationally expensive and time-consuming, especially when dealing with resource-constrained and network-constrained scenarios. Therefore, for analyzing the impact of input data on inference latency, we conducted the inference experiments for the subjects using a representative subset of 100 image samples selected from their specific validation sets with a specific criterion: we ensured that these image samples had larger sizes compared to the remaining validation set. Larger-sized images often present greater computational challenges due to increased memory requirements and processing complexity. By selecting larger-sized image samples, the study can assess an upper bound for the inference latency performance and scalability of the models under investigation in resource-constrained and network-constrained scenarios. The recommendation for a minimum sample size of 100 is considered a typical number for the reliability of statistical analysis and to draw meaningful conclusions [33].

The inference experiment is divided into two stages: trial inference experiment and final inference experiment. For each deployment strategy, a trial inference experiment of 100 sequential inference runs (i.e., inference for 100 input test samples with varying sizes) is conducted to serve as a cache warm-up phase, ensuring that the cache memory is in a steady state before initiating the final inference experiment on the same samples. The cache warm-up phase is intended to mimic real-world deployment scenarios where the model is continuously utilized, and the cache is gradually populated with frequently accessed data instead of performing inference on a cold start. The final inference experiment consists of

---

<sup>5</sup> <https://man7.org/linux/man-pages/man8/tc.8.html>

500 sequential inference runs = 100 (input test samples with varying sizes) x 5 (repetitions). Multiple repetitions are necessary to increase the statistical significance and the reliability of inference latency results. Moreover, it helps capture variability and potential performance fluctuations that may occur during real-world repetitive inference tasks. The inference latency (in seconds) of each inference run in the final inference experiment is logged in a .txt file. After completion of an inference experiment, the simulated mobile, edge, and/or cloud docker containers are restarted to ensure that the next inference experiment is run in a consistent and isolated environment, leading to more reliable and reproducible results. The latency analysis considers models with varying input sizes to simulate dynamic environments.

In our study, the deployment strategies are a mapping of deployment tiers to one or more deployment operators. The deployment tiers are the physical locations for model deployments, which include three single-tier (i.e., mobile, edge, and cloud) and three multi-tier (i.e., mobile-edge, edge-cloud, mobile-cloud) environments. The Single-tiers refer to the deployment of entire models on single computing tiers to achieve monolithic inference. The Multi-tiers refer to the deployment of partitioned models across multiple computing tiers to achieve distributed inference. The deployment operators refer to the specific techniques that are applied to modify black box models for efficient deployment and execution within the Edge AI Environment. They can be categorized into singular operators and hybrid operators. Singular operators are individual optimization techniques that are applied to models independently and Hybrid operators are combinations of singular optimization techniques.

In our study, we considered four singular deployment operators, i.e., Identity Operator (no modifications), Quantization Operator, Early Exit Operator, and Partition Operator. In our study, we explored two hybrid operators, i.e., Quantized Early Exit (QE) and Quantized Early Exit Partition (QEP). We limited the hybrid operators to 2 as developing and evaluating hybrid operators involves combining multiple singular operators, which can increase the complexity of the study. By including a smaller set of hybrid operators, we can perform a more detailed comparative analysis against singular operators.

In our study, we perform Partitioning and Early Exiting manually to check their feasibility (implementation) across the four subject models in ONNX format. The manual feasibility analysis of these operators for ONNX models will help the MLOps Engineers check if it is worth investing time/resources for automating this in the future. For instance, the Early Exiting criteria (i.e., skipping identically structured sub-graphs) require close analysis of ONNX computational graphs of the subject models, as explained in the Early Exiting approach (Section 4.5.3). The Partitioning criteria (i.e., two equal-sized sub-models), require manually checking the sizes of sub-models, while the connection(s) used for achieving this criterion vary for subjects with varying architectures like ResNe(x)t, FCN, and DUC, as explained in our Partitioning approach (Section 4.5.4). Given the heterogeneity of the studied models, there is no automated tool that considers the mentioned criteria for these two operators across all models. To date, only one paper [63], uses a genetic algorithm to evenly split models into diverse sub-models, but this was only evaluated on the ResNet model of our study.

Previous studies [52, 68] indicated that model partitioning does not affect the inference accuracy, it just sends the same intermediate results remotely instead of within the same tier. As the model's architecture inherently involves sequential processing, the partitioning aligns well with this logic by ensuring that data flows through each partitioned model in a manner consistent with the original model's design, hence preserving accuracy. By default, the dimensions (width, height) of the model's input node of three subjects are fixed, i.e., (224, 224) for ResNet/ResNext and (800, 800) for DUC, while for one subject (i.e., FCN), it is dynamic (dependent on the width and height of input data). Therefore, for FCN, the intermediate data dimension/size varies for input data samples having varying widths/heights, while for other subjects, it remains fixed.

The accuracy performance for the other 4 operators (i.e., Identity, Quantization, Early Exit, QE) of each subject is computed independently using their respective validation data set inside the CPU-based docker environments (i.e. mobile, edge), and GPU-based docker environment (i.e., cloud) to assess the impact of the underlying hardware on the operator's performance. Evaluating the accuracy performance inside mobile, edge, and cloud docker containers provides a more comprehensive assessment of the model's generalizability across different hardware platforms. Both mobile and edge docker environments utilize the same Runtime Execution Provider (i.e., CPU) for model inference and have the same processor (Intel(R) Xeon(R) E7-4870, 2.40GHz), but different CPU/Memory configurations.

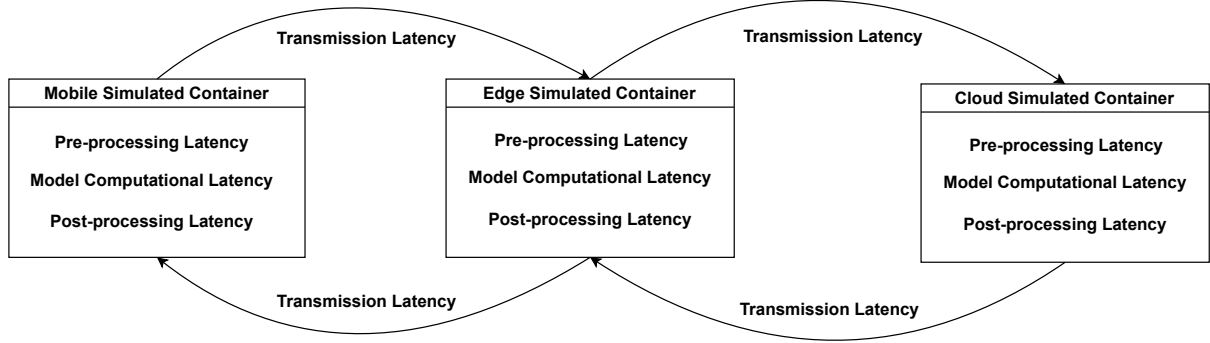


Fig. 3: Graphical illustration of different types of latency contributing to the overall Inference Latency in our experimental setup of 3 containers.

#### 4.4 Metrics for evaluating model performance

##### 4.4.1 Inference Latency

The Inference Latency includes the sum of pre-processing latency, model computational latency, post-processing latency, and transmission latency, as illustrated in Figure 3. The pre-processing latency refers to the time spent transforming input data to align with the requirements of the model. The model computational latency refers to the time it takes to perform the forward pass of a neural network, which involves feeding an input through the network, applying various mathematical operations, and producing an output. The post-processing latency refers to the time spent refining and interpreting the model's output after the model's forward pass. The transmission latency refers to the time it takes for data to travel from one tier to another in an Edge AI network.

The Inference Latency is collected via a timer that is started right before the launch of an inference test run and gets stopped when the model returns the output after successful execution. To that extent, we employ the `default_timer` from the `timeit` python package for measuring inference latency. In the results of the five research questions, we employed the term "speedup" to signify the extent by which the median inference latency of a particular operator or tier is faster compared to the median inference latency of another operator or tier. The median inference latency here is the median value among the five repetitions, where each repetition involves running the inference test over 100 input data samples.

##### 4.4.2 Accuracy

For different domain-specific models, the default accuracy metric varies. In our study, the employed metrics for evaluating the accuracy of image classification subjects like ResNet and ResNext are Top 1% and Top 5% Accuracy, while the metric used for image segmentation subjects like FCN and DUC is mIoU (Mean Intersection Over Union). The definition of the metrics used is as follows:

- Top5% and Top1% Accuracy: Top-5 Accuracy measures the proportion of validation samples where the true label is among the top 5 predictions with the highest confidence score. Top-1 Accuracy is a more strict evaluation metric, as it measures the proportion of validation samples where the model's highest confidence prediction matches the true label. Both Top-1 and Top-5 accuracy are useful metrics in image classification tasks and are often reported together to provide a more comprehensive evaluation of the model's performance. Therefore, in our study, we measure both metrics to gain a better understanding of how well image classification models are performing.
- mIoU%: This is a commonly used metric for evaluating the performance of image segmentation models. It measures the degree of overlap between the predicted segmentation masks and the ground truth masks and provides a measure of how well the model can accurately segment the objects in the image. The mIoU is calculated by first computing the Intersection over Union (IoU) for each class between the predicted mask and the ground truth mask, which is defined as the ratio of the intersection between the predicted and ground truth masks to their union. The IoU ranges from 0 to 1.

1, with higher values indicating better overlap between the predicted and ground truth masks. The mIoU is then calculated as the average of the IoU scores across all classes in the data set.

The reason for using mIoU as an evaluation metric for image segmentation models is that it is sensitive to both false positives (areas predicted as belonging to a class when they do not) and false negatives (areas not predicted as belonging to a class when they should). This makes it a valuable metric for evaluating the overall accuracy of a segmentation model and can help identify areas where the model is performing poorly.

In general, the accuracy metrics were calculated by validating each subject model on its specific validation data set having varying sizes of images to get a more accurate and comprehensive picture of their accuracy performance, as shown in Table 2. The ResNet/ResNext subject models have been validated on the ILSVRC 2012 dataset (50k validation samples), while the FCN and DUC subject models were validated on the COCO 2017 dataset (5k validation samples) and CityScapes leftImg8bit dataset (500 validation samples), respectively. We used "accuracy" as a common term in the RQ results for the 4 subjects' respective accuracy metrics.

#### 4.5 Research Questions

##### 4.5.1 RQ1: What is the performance impact of Monolithic deployment across the tiers of the Edge AI Environment?

*Motivation* This question aims to empirically assess the possible differences in terms of inference performance between the three tiers (i.e., mobile, edge, and cloud) during the monolithic deployment of Identity models (i.e., Identity operator of the subjects). In our study, monolithic deployment on each tier involves deploying an entire model, along with any necessary pre-processing, post-processing, and inference logic, as a single unit. The goal of this research question is to analyze the impact of factors like computational resources, network bandwidth, and input data on inference latency for the 3 monolithic deployment scenarios. The inference accuracy of Identity models is also computed as the baseline for analyzing the performance in later RQs.

*Approach* This approach focuses on running the Inference Experiments for the Identity model of the subjects (i.e., ResNet, ResNext, FCN, DUC) on the individual tiers (i.e., mobile, edge, cloud) for testing and logging the Inference latency. As such, the inference latency experiments are performed on twelve different combinations of <Identity Models(4), Monolithic Deployment tiers(3)>. We evaluate the accuracy of the Identity models on their subject's validation data set, as shown in Table 6.

##### 4.5.2 RQ2: What is the performance impact of the Quantization operator within and across the tiers of the Edge AI Environment?

*Motivation* This question aims to empirically assess the inference latency performance of the quantization operator across two dimensions. In the first dimension, the effectiveness of the quantized models is compared with that of the Identity models of the subjects between corresponding tiers (i.e., mobile, edge, and cloud). In the second dimension, the impact of quantization across the three monolithic tiers (i.e., mobile, edge, and cloud) is analyzed. The inference accuracy of the quantized models is validated and compared with that of the Identity models of the subjects to assess the performance degradation due to quantization.

*Approach* In our study, we used an Intel Neural Compressor (INC) with ONNX Runtime (CPU) backend to perform static PTQ on the subjects. INC is a software tool specifically designed to optimize neural networks for deployment on Intel hardware, such as CPUs or FPGAs. Static PTQ uses a calibration dataset to determine the quantization parameters, such as scaling factors and zero points, for the model. These parameters are essential for representing the floating-point weights and activations of a model in lower-precision fixed-point formats, which are required for quantization. The calibration dataset is used to represent a representative subset of the input data that the model is likely to encounter during inference. For each subject, its validation set is passed as the calibration data to capture the data distribution and help identify appropriate quantization parameters for the model to maintain the desired level of accuracy.

The main advantage of using this technique is that it can lead to a significant reduction in memory requirements and computation time while still maintaining model accuracy. This is especially important in scenarios where the model needs to be deployed on resource-constrained devices, such as mobile or edge devices. In static PTQ, the weights and activations of a pre-trained model are quantized to a fixed precision (i.e., 8-bit integers) by the INC. The Inference Latency Experiments are performed on twelve different combinations of <Quantized Models(4), Monolithic Deployment tiers(3)>. We evaluated the accuracy of the quantized models on their subject's validation dataset as shown in Table 6 and compared the accuracy degradation of quantized models in comparison to the Identity models of the subjects.

#### *4.5.3 RQ3: What is the performance impact of the Early Exiting operator within and across the tiers of the Edge AI Environment?*

*Motivation* Similar to RQ2, this question aims to empirically assess the inference latency performance of the Early Exiting operator across two dimensions. In the first dimension, the effectiveness of the Early Exit models is compared with that of the Identity models of the subjects for corresponding tiers (i.e., mobile, edge, and cloud). In the second dimension, the impact of Early Exiting across the three monolithic tiers (i.e., mobile, edge, and cloud) is analyzed. The inference accuracy of the Early Exit models is validated and compared with the Identity models of the subjects to assess the performance degradation due to Early Exiting.

*Approach* In our study, the early exit process involves modifying the architecture of the pre-trained subjects to include intermediate outputs and adding the necessary logic to allow the models to exit early at an intermediate stage in the neural network, where this stage includes intermediate outputs that can be used for prediction. We create Early Exit models by manually terminating the model early using ONNX python APIs<sup>6</sup>. Since the early exit mechanism damages the accuracy of inference, a relatively slower early exit near the end of the DNN will gain better accuracy performance [99,116]. For this reason, we traverse the ONNX computational graphs for all subjects in reverse order, i.e., starting from the end (output node) to check the sub-graphs having identical structures, then short-circuiting them to create an early exit. Here, the sub-graph denotes a branch network of graphical nodes.

This process takes into account specific considerations related to the model architecture of subjects and the desired trade-off between accuracy and inference speed. When dealing with DNNs, each sub-graph may have specific requirements for the dimensionality of its input and output nodes. If the subsequent sub-graphs have different structures and dimensions, skipping them could lead to incompatible input/output configurations, disrupting the overall flow of the computational process. In our case, the skipping of sub-graphs on each of the subject architectures is based on their identical structure and input/output node dimension. For each of the subjects, we skipped two identical consecutive sub-graphs while traversing from the end. Skipping more than two was not feasible due to the variation in structure as well as the input/output node dimension of the sub-graphs preceding them. Skipping only one sub-graph might not yield a significant speedup, as the reduction in model size would be limited to 1.07x to 1.12x of the Identity models. However, by skipping two consecutive sub-graphs, the model size can be reduced by 1.15x to 1.27x relative to the Identity models, resulting in a more substantial speedup during inference. In the architectures of these subjects (refer to example figure 8 in appendix), there are other sub-graphs (more than 2) having identical structures. Skipping them could result in higher latency as they are placed at the early stages of the graph, which are lighter in weight compared to the ones we selected. For them, skipping a higher number of sub-graphs would be required to yield significant model size reduction and faster latency performance. This would result in significant accuracy loss as these sub-graphs are positioned at the earlier stages of the graph, which capture fundamental features or representations of the input data, which are essential for accurate predictions.

Concretely, on the Identity model of each subject, Algorithm 1 first used the `extract_model()` function to perform the following tasks: 1) Extract an early exit sub-graph having an input node at the start and an early exit point at the end; 2) Extract a decision sub-graph having the early exit point at the start and the output node at the end. The purpose of the decision sub-graph is to make the final prediction based on the information available up to the early exit point. Then, we use the `merge_models()` function to merge the early exit sub-graph with the decision sub-graph. This effectively allows us to either execute

---

<sup>6</sup> <https://github.com/onnx/onnx/blob/main/docs/PythonAPIOverview.md>

the entire model (i.e., the Identity model) or to skip the last 2 consecutive and identical sub-graphs (in terms of structure and input/output node dimension), essentially exiting the model halfway. We provided graphical illustrations of the Early Exiting operation on the ONNX computational graphs of the subjects in Figure 8 9 10.

---

**Algorithm 1** Early Exit based on Sub-Graph Similarity

---

```

1: Input: ONNX computational graph for each subject model
2: Output: Modified computational graph with early exit
3: for each subject model do
4:   Extract the ONNX computational graph  $G_{\text{subject}}$ 
5:   Reverse traverse  $G_{\text{subject}}$  starting from the end
6:   Initialize skip count  $count \leftarrow 0$ 
7:   while not reached the beginning of  $G_{\text{subject}}$  do
8:     Extract current sub-graph  $S_{\text{current}}$ 
9:     Extract preceding sub-graph  $S_{\text{preceding}}$ 
10:    if  $S_{\text{current}}$  has identical structure and input/output dimensions as  $S_{\text{preceding}}$  then
11:      Skip  $S_{\text{current}}$ 
12:      Skip  $S_{\text{preceding}}$ 
13:      Increment  $count$  by 2
14:    else if  $S_{\text{current}}$  doesn't have identical structure and input/output dimensions as  $S_{\text{preceding}}$  then
15:      Break
16:    end if
17:   end while
18:   Remove skipped sub-graphs from  $G_{\text{subject}}$ 
19: end for

```

---

The Inference Latency Experiments are performed on twelve different combinations of <Early Exit Models(4), Monolithic Deployment tiers(3)>. We evaluated the accuracy of the Early Exit models on their subject's validation dataset as shown in Table 6 and compared the accuracy degradation of Early Exit models in comparison to the Identity and Quantized models of the subjects.

#### 4.5.4 RQ4: What is the performance impact of the Partitioning operator across the tiers of the Edge AI Environment?

*Motivation* This research question aims to investigate the impact on inference latency performance of the model partitioning operator across multiple tiers (i.e., mobile-edge, edge-cloud, mobile-cloud) of the Edge AI environment. To understand the effectiveness of the Partitioning operator, this research question also studies the performance comparison of the multi-tier partitioning strategies (i.e., partitioning of Identity models across multiple tiers) with the Monolithic Identity deployment strategies (i.e., Mobile, Edge, and Cloud Deployment of Identity models).

The Partitioned operator in the Mobile-Edge tier is further compared with the other operators (i.e., Identity, Quantization, Early Exit) in the Edge tier. This selection of specific tiers (i.e., Mobile-Edge for Partition and Edge for other operators) is based on the latency advantage they show in comparison to other tiers (i.e., Edge-Cloud/Mobile-Cloud for Partitioning and Mobile/Cloud for other operators).

*Approach* We considered the simple, but effective aspect of equal-size (MB) partitioning to perform a fair evaluation of the subjects. Equal-sized partitioning allows each partitioned model to have a similar level of complexity and workload, which can help to balance the computational load across the tiers of the Edge AI Environment, ignoring the heterogeneity of tiers. This fairness can be crucial for assessing the models objectively and avoiding biases introduced by variations in computational capabilities across tiers or certain tiers being underutilized or overloaded, promoting efficient resource utilization. Moreover, due to the variation in the structural properties of the subjects considered for CV tasks, this straightforward approach might lead to a larger amount of intermediate data being transferred to the MEC network.

For each of the subjects (i.e., ResNet, ResNext, FCN, DUC) considered in our study, we observed that the size of the sub-graphs of the computational graph gradually increases while traversing from the input to the output node. As we progress through the sub-graphs, the receptive field (sensitive to the region of the input image) of nodes expands, incorporating information from a larger context, which often increases the size of the sub-graphs. This observation is consistent with the typical architecture of

DNNs, where lower layers capture low-level features, and higher layers combine these features to form more complex representations. Therefore, choosing the partition point(s) closer to the end might balance the size between the two sub-models, as shown in the partitioning examples in the Appendix.

So, with that in mind, Algorithm 2 inspects the ONNX computational graph of subjects traversing from the end and heuristically selects the partition point, i.e., node connection(s), that splits the model into two nearly equal-sized sub-models. This algorithm is different from the Early Exit algorithm 1 because partitioning focuses on finding the node connection(s) that can partition the model into equal sizes, which requires manually checking the sizes of partitioned models in our study (proof-of-concept algorithm). It deviates from the early exiting approach in which we find and skip identically structured sub-graphs by analyzing their structures and input/output node dimension in ONNX computational graphs.

The models were partitioned so that the connection(s) used for doing that connect the outputs of the 1st half-partitioned model to the input of the 2nd half-partitioned model. For ResNet and ResNext, the connection as shown in Figure 11, available at the start of the 9th sub-graph (from the end), was used as the partitioning point, as it showed the lowest difference in size between the sub-models (i.e, 7-8 MB). These sub-graphs are structured in a way such that one of its branches contains the interconnected nodes and the other branch is a connection (without any interconnected nodes) that eventually merges at the end of the sub-graph. It is not feasible to use the connections within the branches of these sub-graphs for partitioning as it requires each of these branches to have inter-connected nodes to cut the sub-graph.

The architecture of FCN consists of two main branches that extend from the input node and merge at the last sub-graph located at the end. One of the branches consists of all the heavy-weight sub-graphs and the other branch consists mainly of an elongated connection (a connection that spans across the network without containing complex computations or heavy-weight sub-graphs). These two side branches merge into a sub-graph at the end, which computes the final output. Therefore, the partitioning of FCN requires cutting the connection within these two branches to maintain the information flow, as shown in Figure 12. The first connection is situated at the start of the 4th sub-graph from the end within the heavy-weight side branch, and the other connection (within the lightweight side branch) is situated just before the merge. The variation in FCN's partitioned model sizes is limited to 3MB. As explained earlier (for ResNet/ResNext), these sub-graphs lack interconnected nodes in one of their branches, making it unfeasible to use their branches' connections for partitioning.

For DUC, the connection situated at the start of the 4th and 3rd sub-graph from the end shows sub-models with 37 MB and 9MB variation, respectively. The 4th sub-graph from the end contains inter-connected nodes within both its branches and, therefore, cutting the connection within each of its branches can lead to an even more effective balance in size for DUC's sub-models. Therefore, we explored the connections within the branches of this sub-graph and partitioned the DUC model at the connections shown in Figure 13, which resulted in sub-models with around 1MB size variation. This shows that the challenges associated with equal-size partitioning might vary for models with different architectures and therefore manual analysis of their computational graphs and partitioned sub-model sizes is beneficial in such cases.

The manual splitting of the subject's Identity models into two equally sized (in MB) sub-models is performed using ONNX Python APIs. We use the `extract_model()` function on each of the Identity models to perform the following tasks: 1) Extract 1st half of the partitioned model by traversing from the input node to the partition point; 2) Extract 2nd half of the partitioned model by traversing from the partition point to the output node. At the partition point, the output tensor name(s) of the 1st half-partitioned model is identical to the input tensor name(s) of the 2nd half-partitioned model. The 1st half-partitioned sub-model is used for inference in either the mobile or edge tier, while the 2nd half-partitioned sub-model is used for inference in either the edge or cloud tier. The Inference Experiments are performed on twelve different combinations of <Partitioning(4), Multi-tiers(3)>.

#### *4.5.5 RQ5: What is the performance impact of Hybrid Operators within and across the tiers of the Edge AI Environment?*

*Motivation* This question aims to empirically assess the inference latency performance of combining individual operators (i.e., Quantization, Early Exiting, Partitioning) across two dimensions. In the first dimension, the latency and accuracy effectiveness of the Quantized Early Exit (QE) hybrid operator

---

**Algorithm 2** Equal-Size Partitioning of Subject Models

---

```

1: Input: ONNX computational graph  $G_{\text{subject}}$  for each subject model
2: Output: Equal-size partitioned sub-models
3: Initialize Min Size Difference  $\Delta_{\min} \leftarrow \infty$ 
4: Initialize Partition Point  $P \leftarrow \text{null}$ 
5: function PARTITION( $G_{\text{graph}}, \Delta_{\min}, P$ )
6:   Reverse traverse  $G_{\text{graph}}$  starting from the end
7:   while not reached the beginning of  $G_{\text{graph}}$  do
8:     Use connection at the start of the current sub-graph  $S_{\text{current}}$  for partitioning  $G_{\text{graph}}$ 
9:     Calculate size difference  $\Delta$  of partitioned sub-models
10:    if  $\Delta < \Delta_{\min}$  then
11:       $\Delta_{\min} \leftarrow \Delta$ 
12:       $P \leftarrow$  connection at the start of  $S_{\text{current}}$ 
13:    end if
14:   end while
15:   return  $P, \Delta_{\min}$ 
16: end function
17: function PARTITIONRESNE( $x^T(G_{\text{subject}}, \Delta_{\min}, P)$ 
18:    $P, \Delta_{\min} \leftarrow \text{Partition}(G_{\text{subject}}, \Delta_{\min}, P)$ 
19:   return Partitioned sub-models of  $G_{\text{subject}}$  using  $P$  based on  $\Delta_{\min}$ 
20: end function
21: function PARTITIONFCN( $G_{\text{subject}}, \Delta_{\min}, P$ )
22:   Select heavy-weight side branch  $G_{\text{heavy-weight}}$ 
23:   Select light-weight side branch  $G_{\text{light-weight}}$ 
24:    $P \leftarrow$  Use one connection within the  $G_{\text{light-weight}}$  just before the merge for partitioning  $G_{\text{subject}}$ 
25:    $P, \Delta_{\min} \leftarrow \text{Partition}(G_{\text{heavy-weight}}, \Delta_{\min}, P)$ 
26:   return Partitioned sub-models of  $G_{\text{subject}}$  using  $P$  based on  $\Delta_{\min}$ 
27: end function
28: function PARTITIONDUC( $G_{\text{subject}}, \Delta_{\min}, P$ )
29:    $P, \Delta_{\min} \leftarrow \text{Partition}(G_{\text{subject}}, \Delta_{\min}, P)$ 
30:   Reverse traverse  $G_{\text{subject}}$  starting from the end
31:   while not reached the beginning of  $G_{\text{subject}}$  do
32:     if the side branches of the current  $S_{\text{current}}$  contain inter-connected nodes then
33:       Select connections within the branches of the  $S_{\text{current}}$  for partitioning
34:       Calculate size difference  $\Delta$  of partitioned sub-models
35:       if  $\Delta < \Delta_{\min}$  then
36:          $\Delta_{\min} \leftarrow \Delta$ 
37:          $P \leftarrow$  connections within the  $S_{\text{current}}$ 
38:       end if
39:     end if
40:   end while
41:   return Partitioned sub-models of  $G_{\text{subject}}$  using  $P$  based on  $\Delta_{\min}$ 
42: end function

```

---

is compared with the non-partitioned operators (i.e., Identity, Quantization, and Early Exiting) within each monolithic deployment tier (i.e., mobile, edge, and cloud).

In the second dimension, the inference latency impact of the QEP hybrid operator is analyzed across the 3 multi-tiers (i.e., mobile-edge, edge-cloud, mobile-cloud) and that is further compared with the inference latency performance of the hybrid QE operator on monolithic deployment tiers. The QEP hybrid operator in the Mobile-Edge tier is further compared with the non-hybrid operators (i.e., Identity, Quantization, Early Exit) in the Edge tier. The selection of specific tiers (i.e., Mobile-Edge for QEP and Edge for non-hybrid operators) is based on the latency advantage they show in comparison to other tiers (i.e., Edge-Cloud/Mobile-Cloud for QEP and Mobile/Cloud for non-hybrid operators). To analyze model performance degradation, the accuracy of the QE operator is validated and compared with the non-hybrid operators (i.e., Identity, Quantization, and Early Exiting).

Among the 4 non-partitioned operators (i.e., Identity, Quantized, Early Exit, QE), the Identity and QE operators represent the largest and smallest model sizes, respectively. Therefore, the decision to include only the Identity and QE operators for partitioning in RQ4 and in this RQ, respectively, is to focus on variations that demonstrate more pronounced differences in inference latency across the 6 studied tiers. Moreover, the combinations of Partitioning and other operators (such as Early Exiting and Quantization) have already been discussed in previous studies, as stated in related work.(Section 3)

*Approach* This final RQ evaluates the impact of combining the 3 deployment operators (i.e., model quantization, model early exiting, and model partitioning). We perform Early Exiting on the Quantized models by skipping identically structured sub-graphs from the end of the ONNX computational graphs, which is identical to the approach of early exiting in Identity models, as explained in RQ3 (Section 4.5.3). We provided graphical illustrations of the QE operation on the ONNX computational graphs of the subjects as shown in Figure 14 15 16.

We manually partition the QE models into two nearly equal-sized sub-models to generate the QEP operator using a similar procedure as for partitioning of Identity models in RQ4(Section 4.5.4). Here, the 2nd half partitioned model contains the early exit operation, allowing it to make early predictions. The 1st half and 2nd half partitioned sub-models are used for inference in mobile/edge and edge/cloud tier, respectively. We provided graphical illustrations of the QEP operator on the ONNX computational graphs of the subjects as shown in Figure 17 18 19.

The Inference Latency Experiments are performed on 24 different combinations of <Quantize Early Exits (4), Deployment tiers(6)>. The 6 Deployment tiers include 3 single-tiers (i.e., mobile, edge, cloud) and 3 multi-tiers (i.e., mobile-edge, edge-cloud, mobile-cloud). Here, the multi-tier deployment environments involve distributed inference using model partitioning. We evaluated the accuracy of the QE models on their subject’s validation dataset as shown in Table 6 and compared the accuracy degradation of QE models with respect to Identity, Quantize, and Early Existing models of the subjects.

Table 3: Design of KW and Conover statistical tests for inference latency comparison across the Tier(T) dimension, i.e., Mobile[M], Edge[E], Cloud[C], Mobile-Edge[ME], Edge-Cloud[EC], Mobile-Cloud[MC].

T \ O	I	Q	E	P	QE	QEP
M	X					
E	X					
C	X					
ME						
EC						
MC						

(a) RQ1(X)

T \ O	I	Q	E	P	QE	QEP
M		X				
E			X			
C				X		
ME						
EC						
MC						

(b) RQ2(X)

T \ O	I	Q	E	P	QE	QEP
M			X			
E				X		
C					X	
ME						
EC						
MC						

(c) RQ3(X)

T \ O	I	Q	E	P	QE	QEP
M	X					
E	X					
C	X					
ME					X	
EC					X	
MC					X	

(d) RQ4(Y)

T \ O	I	Q	E	P	QE	QEP
M					X,Y	
E					X,Y	
C					X,Y	
ME						Y
EC						Y
MC						Y

(e) RQ5(X) RQ5(Y)

Table 4: Design of KW and Conover test statistical tests for inference latency comparison across the Operator(O) dimension, i.e., Identity(I), Quantization(Q), Early Exiting(E), Partitioned (P), Quantized Early Exiting(QE), and Quantized Early Exiting Partition (QEP)

T \ O	I	Q	E	P	QE	QEP
T	X	X	X		X	
M						
E						
C						
ME			X		X	

(a) Comparison across 6 operators (RQ2, RQ3, RQ4, RQ5)

T \ O	I	Q	E	P	QE	QEP
T	X	X	X		X	
M						
E						
C						
ME				X		X

(b) Comparison across 6 operators (RQ2, RQ3, RQ4, RQ5)

T \ O	I	Q	E	P	QE	QEP
T	X	X	X		X	
M						
E						
C						
ME				X		X

(c) Comparison across 6 operators (RQ2, RQ3, RQ4, RQ5)

## 4.6 Data Analysis

The inference latency experiments' results are analyzed using various statistical methods. Firstly, we use the Shapiro-Wilks test and Q-Q plot for each deployment strategy to assess the normality of the inference latency distribution and determine if parametric or non-parametric tests are appropriate for testing the hypotheses. After observing that the data does not conform to a normal distribution, we employ the Kruskal-Wallis (KW) test [81] to compare the inference latency distributions of independent groups (i.e., deployment strategies) based on two different dimensions (i.e., operator and tier dimension) and determine if there exists a significant difference among at least two of the independent groups (hypothesis testing). The design approach for the KW and Conover statistical tests across the tier and operator Dimension is illustrated in Table 3 and Table 4, respectively.

### 4.6.1 Tier Dimension

As shown in Table 3, to investigate if there is a statistically significant difference between the 3 monolithic deployment tiers (single-tiers) in terms of inference latency of any of the non-partitioned operators, we perform a KW test ( $\alpha = 0.05$ ) for each of the 4 Identity models in RQ1, 4 Quantized models in RQ2, 4 Early Exit models in RQ3, and 4 QE models in RQ5 by comparing their latency across the 3 single-tiers (Mobile, Edge, Cloud). Moreover, to investigate if there is a statistically significant difference between the Monolithic deployment strategies and Multi-tier Partitioning strategies, for each subject, we conduct a KW test ( $\alpha = 0.05$ ) across the Identity and Partitioned models in RQ4. We also perform this test across the QE and QEP models in RQ5, on their inference latency performance when deployed in the 3 single-tier and 3 multi-tier environments, respectively.

After observing significant differences (KW Test: p-value < 0.05), we further employ the Conover post-hoc test [12]. For the pairwise comparisons having significant differences (Conover test: adjusted p-value < 0.05), we evaluate Cliff's delta effect size [10] to assess the inference latency ranking of tiers based on the direction and magnitude of their difference in the corresponding RQs.

### 4.6.2 Operator Dimension

For each subject, to investigate if there is a statistically significant difference between the 6 operators (Identity, Quantized, Early Exit, Partitioned, QE, QEP), we perform the KW tests shown in Table 4. If there is a significant difference (KW Test: p-value < 0.05), we further employ post-hoc Conover tests [12]. For the pairwise comparisons having significant differences (Conover test: adjusted p-value < 0.05), we

used Cliff's delta effect size [10] to analyze how operators' inference latency ranks by looking at how much they differ (magnitude) and which way (sign) they differ in the corresponding RQs.

To evaluate the accuracy comparisons of the operators, we use the Wilcoxon Signed Rank Test [18] to determine if there exists a significant difference for the Identity vs Quantized models in RQ2, Identity vs Early Exit models in RQ3, Quantized vs QE models in RQ4, and Early Exit vs QE models in RQ5. This test analyzes the differences between 2 paired groups, i.e., the accuracy measurements under 2 different operators for the same subjects (i.e., ResNet, ResNext, FCN, DUC) and environments (i.e., Mobile, Edge, Cloud). Each group has 18 samples of accuracy measurements, i.e., 6 accuracy metric values ([ResNet, ResNext] x [Top 1%, Top 5%] + [FCN, DUC] x [mIOU%]) x 3 environments. In other words, in a particular operator's group, we are concatenating the accuracy metric(s), all of which are percentage values, of all four subjects, then comparing corresponding accuracy metrics using paired statistical tests.

To avoid false discoveries, Bonferroni Correction [38] is applied to the p-value for each Wilcoxon test comparing 2 operators by considering a p-value less than or equal to 0.0125 as statistically significant. The adjusted significance level of 0.0125 is derived by dividing the conventional significance level ( $\alpha = 0.05$ ) by the number of multiple comparisons (4 in our case, as each operator is compared four times). After this correction, if a significant difference is observed between the 2 operators, we utilize Cliff's Delta effect size [10] to measure the magnitude/sign of their difference in corresponding RQs.

On the other hand, for the Shapiro-Wilks, Kruskal-Wallis, and Posthoc Conover tests, we compare the obtained p-value with the significance level of alpha = 0.05. According to [37], we interpret effect size as negligible ( $d < 0.147$ ), small ( $0.147 \leq d < 0.33$ ), medium ( $0.33 \leq d < 0.474$ ), or large ( $d \geq 0.474$ ). Negative values for  $d$  imply that, in general, samples from the distribution on the left member of the pair had lower values. These findings, in combination with the box plots displaying the distributions, will provide us with an additional understanding of the extent to which one deployment strategy differs from another. In particular, we analyze the median in the box plots to evaluate how each deployment strategy's performance compares to the others.

## 5 Results

5.1 What is the impact of monolithic deployment tiers in an Edge AI Environment? (RQ1)

**For the Identity models having large input data sizes (ResNet, ResNext, and DUC), the Edge tier shows the lowest median inference latency of 5.64, 3.96, and 23.64 seconds, respectively.**

The box plots in Fig. 4 represent the Inference Latency distribution in the logarithmic scale of the subject's Identity models across the mobile, edge, and cloud tiers. The Conover test shows significant differences in all pairwise comparisons between the three monolithic deployment tiers for each identity model. The Edge tier shows a 3.12x, 4.43x, and 1.21x lower median inference latency compared to the cloud tier for ResNet, ResNext, and DUC Identity models, respectively with a large effect size (Table 5). This is because of the Edge's higher network bandwidth capacity (200 Mbps) compared to Cloud (1Mbps), which allows faster transmission of large input data samples for ResNet/ResNext (8 to 60Mb) and DUC (19-22Mb) during Edge deployment.

In contrast, the FCN Identity model shows the lowest median inference latency of 3.76 seconds in the Cloud tier, while the other 3 Identity models show the highest median inference latency of 17.61, 17.61, and 28.61 seconds, respectively in the Cloud tier. This is because the input data samples for FCN are much smaller in size (2-5 Mb), which allows faster data transmission even in the network-constrained cloud tier. Moreover, the Interquartile range (IQR) of the ResNet and ResNext is wider compared to FCN and DUC in the Cloud, indicating a more significant variability around the median. This is because the input data size range of ResNet and ResNext is around 17x higher compared to FCN and DUC, so a higher spread of inference latency values is observed for ResNet and ResNext. This behavior indicates that the input data sizes and network bandwidths play a critical role in the end-to-end inference latency during edge and cloud deployment.

The Edge tier shows 1.83x lower average median inference latency compared to the Mobile tier across the four identity models. In particular, the edge shows a drop of 3.30, 2.33, 15.10, and 21.81 seconds in median inference latency compared to mobile for ResNet, ResNext, FCN, and DUC Identity models, respectively along with a large effect size (Table 5). These differences are possibly due to the larger

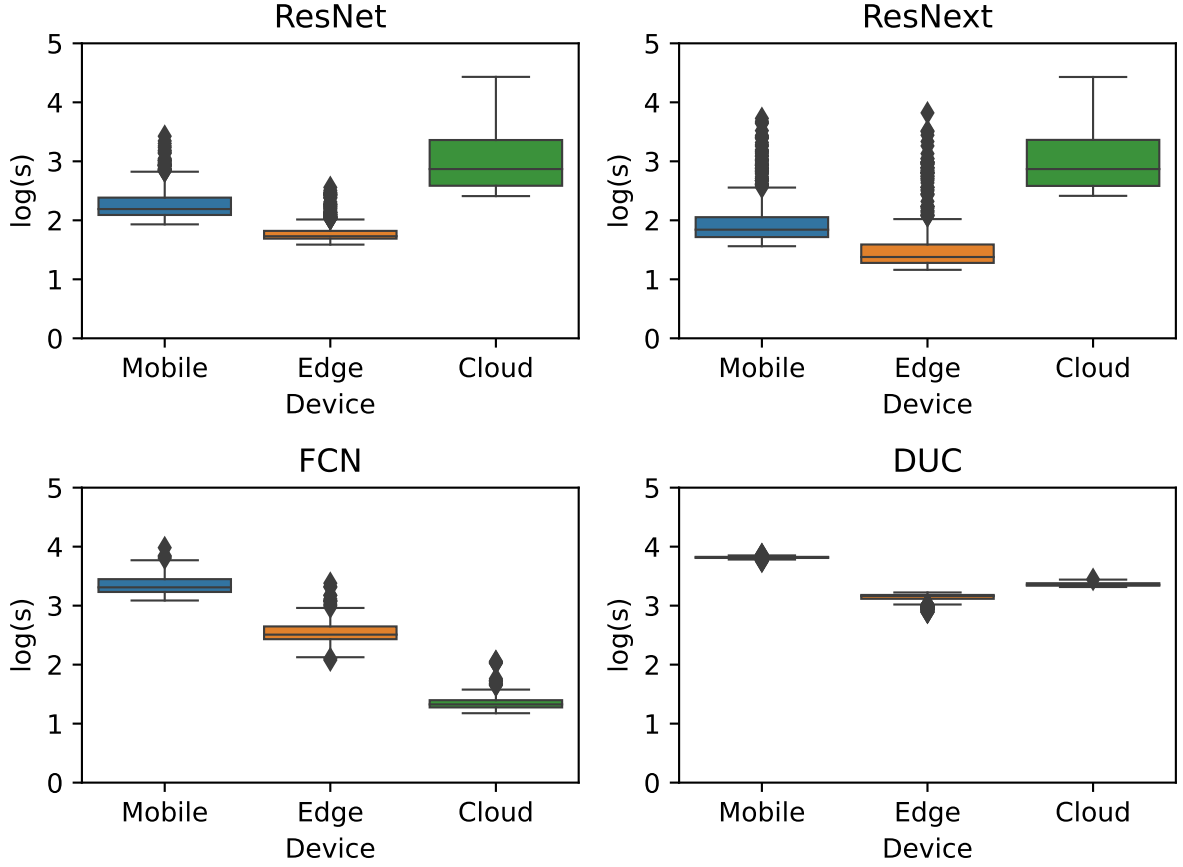


Fig. 4: Box plots of the measures collected for Inference Latency from Mobile, Edge, and Cloud tiers for Identity versions of Subjects

computational resources (CPU/RAM) of the edge tier compared to the mobile tier, due to which the computations during model inference are faster in the Edge tier. In particular, Edge has 4x the RAM and twice as many CPU cores as mobile. The Cloud tier shows an 8.52 and 23.62 seconds drop in median inference latency compared to both mobile and edge tiers, respectively only for the FCN Identity model as the abundant computational resources of the cloud (16x/4x RAM and 4x/2x CPU relative to Mobile/Edge) and the lowest input data size range for the FCN subject (as mentioned earlier) accounts for both faster model inference and data transmission.

The architectural complexity of models also plays a role in inference as among the 4 Identity models, the DUC Identity model shows the highest median inference latency of 45.46, 23.64, and 28.61 seconds on Mobile, Edge, and Cloud, respectively. The DUC Identity model has the highest number of graph nodes (i.e., 355), which contributes to the higher architectural complexity in comparison to the other Identity models (FCN: 260 graph nodes, ResNet/ResNext: 240 graph nodes). Here, the graph nodes represent the total number of operations in the ONNX computational graph of a model.

After rounding off the decimal digits (up to 4 places) in the accuracy metric values, we observed that for each subject, each of the 4 operators (i.e., Identity, Quantized, Early Exit, and QE) exhibits almost identical performance between mobile and edge tiers, as shown in Table 6. The main reason seems to be the identical hardware (CPU processor) and software (packages) configuration of mobile and edge-simulated docker containers.

Table 5: RQ1 Results of the Cliff's Delta effect size between Mobile (M), Edge (E), and Cloud (C) Deployment for  $I_t$  (Identity version of ResNet),  $I_x$  (Identity version of ResNext),  $I_f$  (Identity version of FCN), and  $I_d$  (Identity version of DUC).

$I_x \setminus I_t$	M	E	C
M	-	L	-L
E	L	-	-L
C	-L	-L	-

$I_d \setminus I_f$	M	E	C
M	-	L	L
E	L	-	L
C	L	-L	-

<sup>1</sup> In these, and later, tables, a Positive sign for the  $i^{th}$  cell shows that the latency of column[i]<row[i], while a Negative sign for the  $i^{th}$  cell shows that the latency of column[i]>row[i].

<sup>2</sup> In these, and later, tables, the L, M, S, and N symbols mean Large, Medium, Small, and Negligible effect size, respectively.

<sup>3</sup> In these, and later, tables, an empty cell means that the cliff's delta effect size was not considered because the pairwise comparison was not statistically significant based on the Conover test.

Table 6: Accuracy Performance of Identity, Quantized, Early Exit, and QE versions of Subjects within Mobile, Edge, and Cloud tiers.

Subject	Operator	Model Size	Top-1%			Top-5%			mIOU%		
			Mobile	Edge	Cloud	Mobile	Edge	Cloud	Mobile	Edge	Cloud
ResNet	Identity	484 MB	82.52	82.520	82.522	96.008	96.008	96.008	-	-	-
ResNet	Quantized	123 MB	82.148	82.148	82.164	95.792	95.792	95.814	-	-	-
ResNet	Early Exit	380 MB	76.586	76.586	76.59	93.442	93.442	93.446	-	-	-
ResNet	Quantized Early Exit	96 MB	75.392	75.392	75.346	93.034	93.034	93.024	-	-	-
ResNext	Identity	319 MB	83.244	83.244	83.244	96.456	96.456	96.458	-	-	-
ResNext	Quantized	81 MB	83.084	83.084	83.14	96.402	96.402	96.386	-	-	-
ResNext	Early Exit	250 MB	77.276	77.276	77.284	93.92	93.92	93.924	-	-	-
ResNext	Quantized Early Exit	64 MB	75.668	75.668	75.616	93.83	93.83	93.826	-	-	-
FCN	Identity	199 MB	-	-	-	-	-	-	66.7343	66.7343	66.7348
FCN	Quantized	50 MB	-	-	-	-	-	-	66.38	66.38	66.35
FCN	Early Exit	164 MB	-	-	-	-	-	-	55.16	55.16	55.16
FCN	Quantized Early Exit	42 MB	-	-	-	-	-	-	54.36	54.36	54.32
DUC	Identity	249 MB	-	-	-	-	-	-	81.9220	81.9220	81.9223
DUC	Quantized	63 MB	-	-	-	-	-	-	81.62	81.62	81.62
DUC	Early Exit	215 MB	-	-	-	-	-	-	75.746	75.746	75.744
DUC	Quantized Early Exit	54 MB	-	-	-	-	-	-	75.32	75.32	75.32

### Summary of Research Question 1

Among the three monolithic deployment tiers, the Edge tier could be the preferred choice in terms of latency in scenarios where models (ResNet, ResNext, DUC) have large input data size requirements and the Mobile/Cloud tier has computational/bandwidth limitations. In contrast, for models having smaller input data size requirements (FCN), cloud deployment could be the optimal choice over computationally constrained tiers (Mobile/Edge).

### 5.2 What is the impact of the Quantization operator within and across the tiers of the Edge AI Environment (RQ2)

In Mobile, the Quantized models show 1.17x higher and 1.27x lower average median inference latency w.r.t identity models for ResNet/Resnext and FCN/DUC, respectively. In Edge, the Quantized models show 1.48x lower average median inference latency than the Identity models across all subjects. In the cloud, no significant difference was shown among Quantized and Identity models across all subjects (except DUC).

As shown in Figure 5 (blue and orange box plots), the Quantized models show 1.15x to 1.19x higher and 1.17x to 1.37x lower median inference latency compared to the Identity models in the mobile tier, along with small to large effect sizes (Table 7). The generated Quantized models are about 4x smaller than the Identity models of the subjects as shown in Table 6. Therefore, in an ideal situation the Quantized

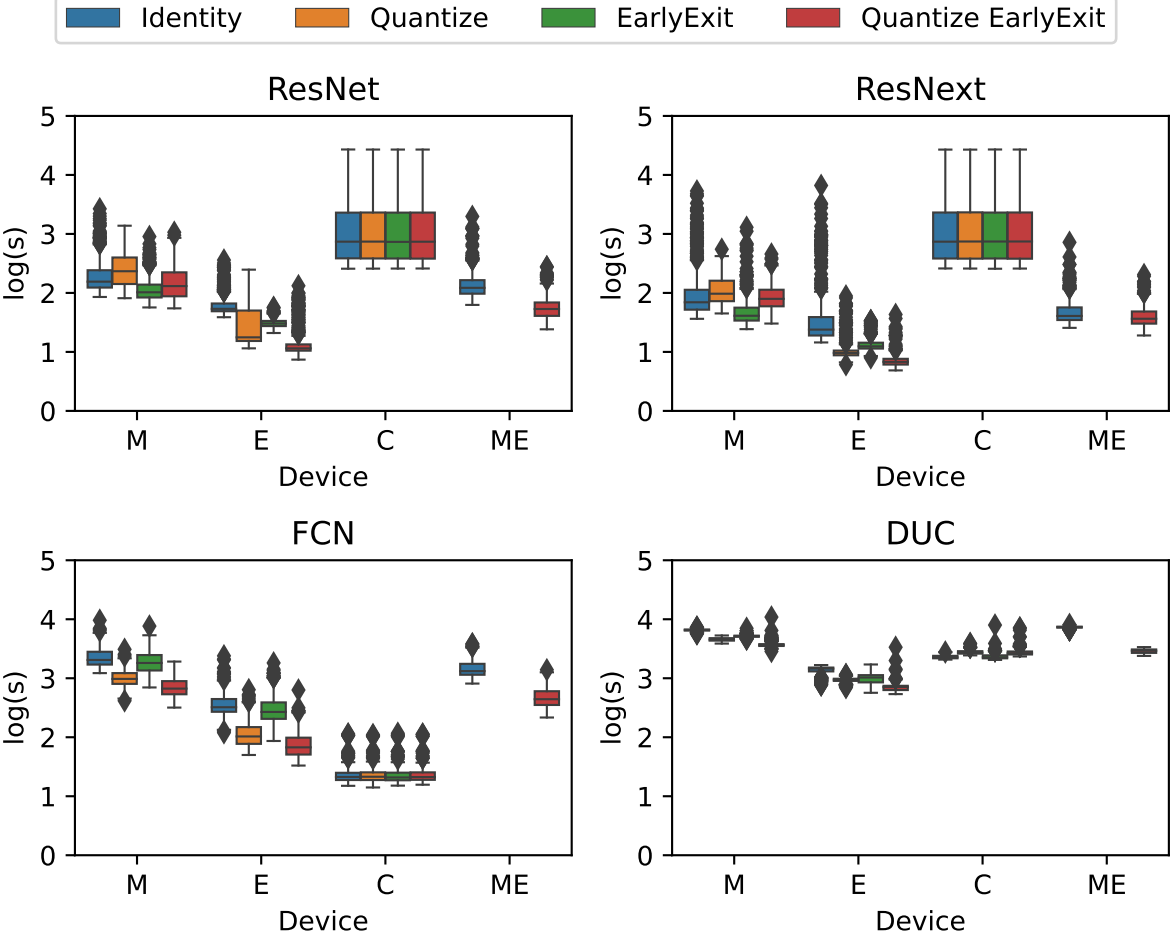


Fig. 5: Box plots of the measures collected for Inference Latency of Identity, Quantized, Early Exit, QE models in monolithic tiers and Partitioned Identity/QE models in Mobile-Edge (ME) tier.

models should show faster latency in comparison to identity models due to model size reduction, as shown in FCN and DUC’s latency results. But, for the ResNet and ResNext subjects, these models show slower latency possibly due to their costly operations in the resource-constrained mobile tier, leading to their higher CPU/Memory utilization than Identity models. In the Edge tier, the Quantized models show 1.20x to 1.64x lower median inference latency than the identity models across the four subjects along with large effect sizes (Table 8). This shows that the Quantized models perform faster than the identity models in a high-resource environment (i.e., edge).

According to the Conover test, the null hypothesis that there is no significant inference latency difference between the Quantized and Identity models was rejected for the DUC subject ( $2.0e^{-247}$ ,  $\alpha = 0.05$ ) during cloud deployment. The large effect size (Table 9) for DUC shows that its Quantized model has a significantly higher distribution of inference latency magnitude compared to its Identity model. Conversely, for the remaining three subjects (i.e., ResNet, ResNext, FCN), the null hypothesis cannot be rejected indicating that their Quantized models show similar or equivalent inference latency compared to their Identity models.

During Cloud inference, the majority of graphical nodes (94.01% to 100%) are processed on the CUDA Execution provider for the Identity models, while for the Quantized models, 53.82% to 86.52% of the graphical nodes are processed on the CUDA Execution Provider and the remaining ones are processed on the CPU Execution Provider. Compared to Identity models, the percentage of graphical nodes that use CUDA Execution Provider is lower for Quantized models, which might imply that Quantized models are somewhat less optimized (or compatible) for GPU (i.e., CUDA) processing than identity models. Among

the four subjects, the Quantized model of DUC shows the lowest percentage of the graphical nodes (53.82%) placed on the CUDA Execution Provider resulting in its significantly slower inference latency than the DUC Identity model, for which all the graphical nodes are placed on the CUDA execution provider. For the remaining three subjects (i.e., ResNet, ResNext, FCN), the Quantized models show similar inference latency compared to the identity models in the Cloud tier due to the higher percentage of graphical nodes placed on the CUDA execution provider, i.e., 85.62% to 86.52% and 94.01% to 100% for Quantized and identity models respectively.

**The Quantized models show a small accuracy drop of 0.05% to 0.38% across the four subjects in comparison to identity models.**

In terms of accuracy, the Quantized models demonstrate a marginal accuracy drop of 0.05% down to 0.38% compared to the Identity models, as shown in Table 6. The Wilcoxon test confirms the significance of this accuracy drop ( $p\text{-value} = 7.6e^{-6}$ ,  $\alpha = 0.0125$ ). However, the effect size remains small (0.16). This trade-off suggests that Quantization is an effective operator for achieving faster inference in Edge (based on previous findings) without significantly compromising the accuracy performance.

**When comparing Quantization across the three monolithic deployment tiers, the Quantized models show 2.60x and 3.44x lower average median inference latency during Edge deployment than their deployment in Mobile and Cloud, respectively.**

The Quantized models across all subjects in the Edge exhibit 1.97x to 3.06x lower median inference latency compared to their inference in the Mobile, as shown in Figure 5 (orange boxplots), along with large effect sizes (Table 10) due to its higher computational resources. For ResNet, ResNext, and DUC subjects, the Quantized models in the Cloud demonstrate 1.58x to 6.61x higher median inference latency than their inference in the Edge tier due to the higher impact of the large input data sizes of these subjects on the transmission across the restricted edge-cloud network. However, the Quantized model for the FCN subject exhibits 1.97x lower median inference latency in the Cloud tier compared to the Edge tier with a large effect size (Table 10). This is due to the FCN’s small input data sizes leading to a lower impact on data transmission across the restricted edge-cloud network. The reasoning behind these findings is similar and explained briefly in the RQ1 findings (Section 5.1).

Table 7: Cliff’s Delta effect size between  $I_M$ ,  $Q_M$ ,  $E_M$ ,  $P_{ME}$ ,  $QE_M$ , and  $QEP_{ME}$  versions of subjects for RQ2, RQ3, RQ4, and RQ5

ResNet \ ResNext		$I_M$	$Q_M$	$E_M$	$P_{ME}$	$QE_M$	$QEP_{ME}$
$I_M$	-	-S	L	M	S	L	
$Q_M$	-M	-	L	L	M	L	
$E_M$	L	L	-	-S	-S	L	
$P_{ME}$	L	L		-		L	
$QE_M$	-N	S	-L	-L	-	L	
$QEP_{ME}$	L	L	S	S	L	-	

FCN \ DUC		$I_M$	$Q_M$	$E_M$	$P_{ME}$	$QE_M$	$QEP_{ME}$
$I_M$	-	L	S	L	L	L	
$Q_M$	L	-	-L	-L	L	L	
$E_M$	L	-L	-	M	L	L	
$P_{ME}$	-L	-L	-L	-	L	L	
$QE_M$	L	L	L	L	-	L	
$QEP_{ME}$	L	L	L	L	L	-	

<sup>1</sup>  $I_M$ ,  $Q_M$ ,  $E_M$ ,  $QE_M$  denotes Identity, Quantized, Early Exit, Quantized Early Exit models in Mobile tier.

<sup>2</sup>  $P_{ME}$  and  $QEP_{ME}$  denotes Partitioned and Quantized Early Exit Partition models in the Mobile-Edge tier.

Table 8: Cliff's Delta effect size between  $I_E$ ,  $Q_E$ ,  $E_E$ ,  $P_{ME}$ ,  $QE_E$ , and  $QEP_{ME}$  versions of subjects for RQ2, RQ3, RQ4, and RQ5

ResNet		$I_E$	$Q_E$	$E_E$	$P_{ME}$	$QE_E$	$QEP_{ME}$
ResNext	$I_E$	-	L	L	-L	L	N
	$Q_E$	L	-		-L	L	-L
	$E_E$	L	-L	-	-L	L	-L
	$P_{ME}$	-L	-L	-L	-	L	L
	$QE_E$	L	L	L	L	-	-L
	$QEP_{ME}$	-M	-L	-L	S	-L	-

FCN		$I_E$	$Q_E$	$E_E$	$P_{ME}$	$QE_E$	$QEP_{ME}$
DUC	$I_E$	-	L	S	-L	L	-L
	$Q_E$	L	-	-L	-L	L	-L
	$E_E$	L	-S	-	-L	L	-L
	$P_{ME}$	-L	-L	-L	-	L	L
	$QE_E$	L	L	L	L	-	-L
	$QEP_{ME}$	-L	-L	-L	L	-L	-

<sup>1</sup>  $I_E$ ,  $Q_E$ ,  $E_E$ ,  $QE_E$  denotes Identity, Quantized, Early Exit, Quantized Early Exit models in Edge tier.

<sup>2</sup>  $P_{ME}$  and  $QEP_{ME}$  denotes Partitioned and Quantized Early Exit Partitioned models in Mobile-Edge tier.

Table 9: Cliff's Delta effect size between  $I_C$ ,  $Q_C$ ,  $E_C$ ,  $P_{ME}$ ,  $QE_C$ , and  $QEP_{ME}$  versions of subjects for RQ2, RQ3, RQ4, and RQ5

ResNet		$I_C$	$Q_C$	$E_C$	$P_{ME}$	$QE_C$	$QEP_{ME}$
ResNext	$I_C$	-			L		L
	$Q_C$		-		L		L
	$E_C$			-	L		L
	$P_{ME}$	L	L	L	-	-L	L
	$QE_C$				-L	-	L
	$QEP_{ME}$	L	L	L	S	L	-

FCN		$I_C$	$Q_C$	$E_C$	$P_{ME}$	$QE_C$	$QEP_{ME}$
DUC	$I_C$	-			-L		-L
	$Q_C$	-L	-		-L		-L
	$E_C$	-N	L	-	-L		-L
	$P_{ME}$	-L	-L	-L	-	L	L
	$QE_C$	-L	S	-L	L	-	-L
	$QEP_{ME}$	-L	-S	-L	L	-M	-

<sup>1</sup>  $I_C$ ,  $Q_C$ ,  $E_C$ ,  $QE_C$  denotes Identity, Quantized, Early Exit, Quantized Early Exit models in Cloud tier.

<sup>2</sup>  $P_{ME}$  and  $QEP_{ME}$  denotes Partitioned and Quantized Early Exit Partitioned models in Mobile-Edge tier.

Table 10: RQ2 Results of the Cliff's Delta effect size between Mobile (M), Edge (E), Cloud (C) Deployment of Quantized models ( $Q_t$ ,  $Q_x$ ,  $Q_b$ ,  $Q_r$  denotes Quantized versions of ResNet, ResNext, FCN, DUC)

$Q_t$		M	E	C
$Q_x$	$Q_t$			
	M	-	L	-L
	E	L	-	-L
C	-L	-L	-	

$Q_f$		M	E	C
$Q_d$	$Q_f$			
	M	-	L	L
	E	L	-	L
C	L	-L	-	-

## Summary of Research Question 2

The Quantization operator could be the preferred choice over the Identity operator across the four subjects when faster latency (1.48x) is a concern in the Edge tier, at a small accuracy loss (<0.4%). Among the three monolithic deployment tiers, the Edge again is the most suitable deployment tier for the Quantization operator when factors like large input data size and constrained computational (Mobile)/ network (Cloud) environment play a crucial role. In contrast, Cloud deployment again is a better option for this operator when factors like small input data sizes and constrained computational environments (Mobile/Edge) are important.

5.3 What is the performance impact of the Early Exit operator within and across the tiers of the Edge AI Environment? (RQ3)

**In Mobile and Edge, the Early Exit models show a 1.15x and 1.21x lower average median inference latency than the Identity models, respectively. In the Cloud, the Early Exit models show no practically significant difference in inference latency compared to the Identity models.**

The Early Exit models show 1.05x to 1.25x and 1.08x to 1.32x lower median inference latency than the Identity models in the mobile and edge tiers, respectively, as shown in Figure 5 (blue and green boxplots), along with small or large effect sizes (Table 7 and Table 8). The utilization of intermediate predictions in the Early Exit models allows it to leverage information from earlier stages of the neural network, leading to model size reduction (1.15x to 1.27x) and faster inference compared to the Identity models in restricted-constrained tiers (i.e., mobile and edge).

According to the Conover test, for ResNet, ResNext, and FCN, the null hypothesis that there is no significant difference between the Early Exit and Identity model in the Cloud cannot be rejected, indicating that the Early Exit models during Cloud deployment show similar or equivalent inference latency compared to the Identity models. For the DUC subject, the null hypothesis was rejected, although with a negligible effect size (Table 9), suggesting that the difference is likely not practically significant. The main reason for not having a significant difference is the ample availability of computational resources in the Cloud tier compared to resource-constrained mobile and edge tiers due to which the impact of Early Exiting on subjects is not significant in comparison to the Identity models in the Cloud tier.

**In Mobile, the Quantized models show 1.44x higher and 1.18x lower average median inference latency w.r.t Early Exit models for ResNet/ResNext and FCN/DUC, respectively. In Edge, the Quantized models show 1.23x lower average median inference latency than the Early Exit models across the four subjects. In Cloud, no significant inference latency difference was shown among Quantized and Early Exit models across all subjects (except DUC).**

During Mobile deployment, the Quantized models for ResNet and ResNext subjects show 1.42x to 1.45x higher median inference latency than the Early Exit models as shown in Figure 5 (orange and green box-plots), along with large effect sizes (Table 7). In contrast, for FCN and DUC subjects, the Quantized models show 1.05x to 1.31x lower median inference latency than the Early Exit models, along with large effect sizes (Table 7). Even though the Quantized model sizes of the ResNet and ResNext subjects are 3.08x lower than the Early Exit models, they still show slower latency results, possibly due to the costly quantization operations of these two subjects in a low-resource environment (i.e., mobile) similar to the reasoning discussed in RQ1 (Section 5.1) when comparing Quantized models with Identity models in the mobile tier.

In the Edge tier, the Quantized models show 1.03x to 1.51x lower median inference latency than the Quantized models across the four subjects. In comparison to Early Exit models (Table 8), the inference latency of Quantized models is similar (ResNet) or significantly faster with small (DUC) or large (ResNext, FCN) effect sizes. This shows that in the edge tier, the Quantized models are overall a better option than the Early Exit models in terms of faster latency.

In the Cloud tier, the Quantized models show no statistically significant difference (according to the Conover test) in inference latency in comparison to Early Exit models for all subjects (except DUC). The reasoning for these findings is due to the lower compatibility of DUC's quantization nodes with the

CUDA Execution Provider during Cloud deployment, which is similar to those discussed briefly in the first finding of RQ1 (Section 5.1) when comparing Quantized and Identity models in the Cloud tier.

**The Early Exit models cost a medium accuracy drop of 2.53% to 11.56% and 2.35% to 11.21% in comparison to Identity and Quantized models, respectively.**

In terms of accuracy, the Early Exit models show a significant statistical difference (Wilcoxon Test:  $p\text{-value} = 7.6e^{-6}$ ,  $\alpha = 0.0125$ ) with a medium effect size (0.38) in comparison to Identity and Quantized models. As presented in Table 6, the Early Exit models reveal an accuracy drop ranging from 2.53% to 11.56% and 2.35% to 11.21% when compared with Identity and Quantized models. This finding suggests that Early Exit models are less effective in accuracy performance relative to both Identity and Quantized models. Based on this and previous findings, the quantization operator can achieve faster inference while maintaining a reasonably high level of accuracy, making it a preferred choice over the early exit operator.

**When comparing Early Exiting across the three Monolithic deployment tiers, the Early Exit models show 1.92x and 2.90x lower average median inference latency during Edge deployment than their deployment in Mobile and Cloud tiers, respectively.**

The Early Exit models in the Edge outperform the ones on the Mobile tier by 1.69x to 2.29x in terms of median inference latency, as shown in Figure 5 (green boxplots), with large effect sizes (Table 11) due to the higher computational resources of Edge. For ResNet, ResNext, and DUC subjects, the Early Exit models in the Cloud tier exhibit 1.40x to 5.91x higher median inference latency compared to the Edge, with large effect sizes (Table 11) due to the higher impact of the large input data sizes of these subjects on the transmission across the restricted edge-cloud network during cloud deployment. However, for the FCN subject, the Early Exit model in the Cloud tier experiences a 3.03x lower median inference latency compared to the Edge tier, with a large effect size (Table 11). This is due to the FCN's small input data sizes leading to a lower impact on data transmission across the restricted edge-cloud network during cloud deployment. The reasoning behind these findings is similar and explained briefly in the RQ1 findings (Section 5.1).

Table 11: RQ3 Results of the Cliff's Delta effect size between Mobile (M), Edge (E), and Cloud (C) Deployment of Early Exit models.

$E_t$ $E_x$	M	E	C
M	-	L	-L
E	L	-	-L
C	-L	-L	-

$E_f$ $E_d$	M	E	C
M	-	L	L
E	L	-	L
C	L	-L	-

<sup>1</sup>  $E_t$ ,  $E_x$ ,  $E_f$ ,  $E_d$  denotes Early Exit versions of ResNet, ResNext, FCN, and DUC.

### Summary of Research Question 3

Similar to RQ2, the Quantized operator could be the preferred choice when faster latency (1.23x) is a concern in the Edge tier, at medium accuracy improvement (up to 11.21%) than the Early Exit operator, which shows faster latency (1.21x) than the Identity models at medium accuracy drop (up to 11.56%). Among the three monolithic deployment tiers, the Edge again is the most suitable deployment tier for the Early Exit operator when factors like large input data size and constrained computational (Mobile)/ network(Cloud) environment play a crucial role. Cloud deployment is again a better option for this operator when factors like small input data size and constrained computational environments (Mobile/Edge) play a crucial role.

5.4 What is the impact of the Partitioning operator across the tiers of the Edge AI Environment? (RQ4)

**Among the three Multi-tier Partitioning strategies, the Mobile-Edge Partitioning strategy shows 9.37x and 9.86x lower average median inference latency compared to Edge-Cloud and Mobile-Cloud Partitioning strategies, respectively.**

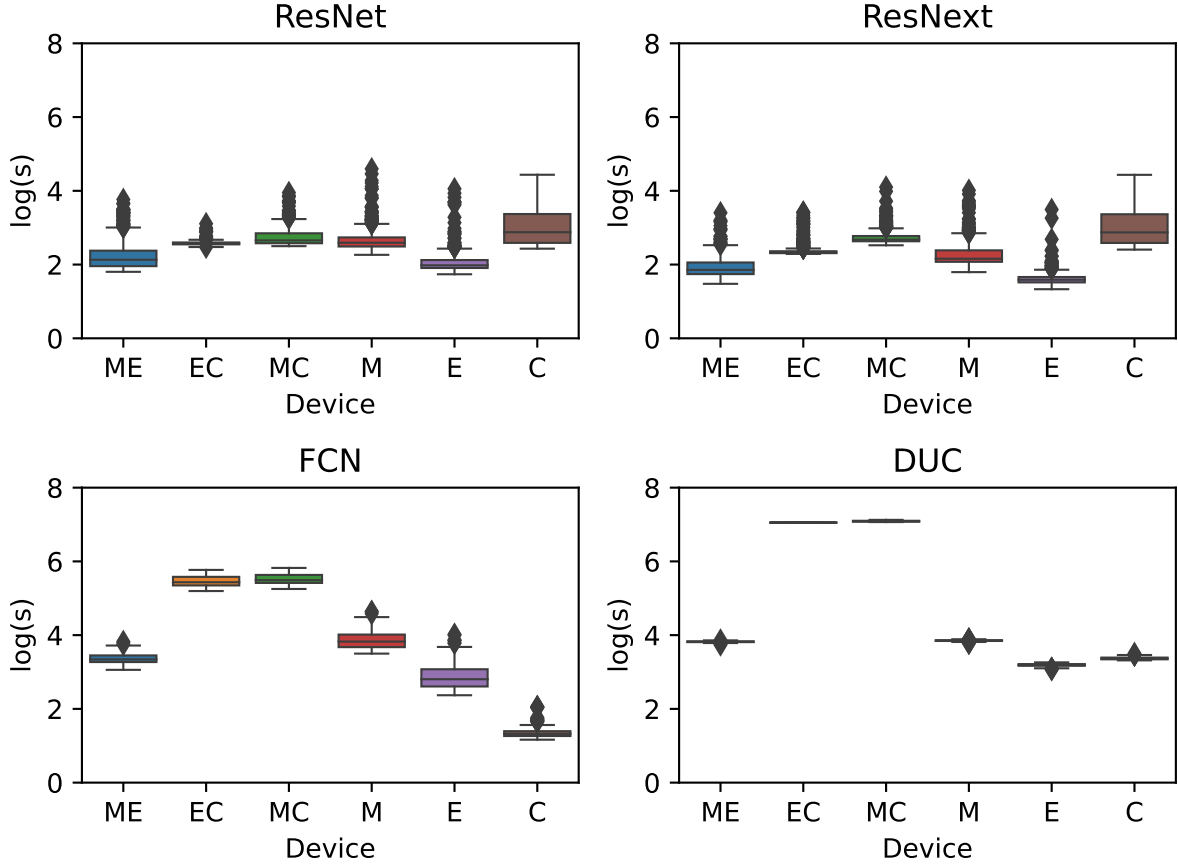


Fig. 6: Box plots of the Inference Latency measure for Multi-tier (Mobile-Edge [ME], Edge-Cloud [EC], Mobile-Cloud [MC]) Partitioning strategies and Single-tier (Mobile[M], Edge[E], Cloud[C] Monolithic Deployment strategies

The Mobile-Edge Partitioning strategy outperforms the Edge-Cloud and Mobile-Cloud Partitioning strategies in terms of median inference latency as depicted in Figure 6 (blue, orange, and green box-plots). In particular, it achieves a significant speedup, ranging from 1.37x to 24.17x and 1.74x to 24.95x compared to the Edge-Cloud and Mobile-Cloud Partitioning strategies, respectively, with large effect sizes (Table 12).

The primary reason for this behavior is the impact of the size of intermediate data during transmission across the edge-cloud network. In the Edge-Cloud and Mobile-Cloud Partitioning strategies, the intermediate results generated after the first half of inference need to be transmitted from the edge tier to the cloud tier for the second half of inference. This transmission incurs additional latency, particularly when the intermediate data size of subjects (i.e., 6.12Mb for ResNet/ResNext, 118.12 to 200Mb for FCN, 781.25Mb for DUC) is larger than the limited cloud Network bandwidth (1 Mbps). Conversely, the Mobile-Edge Partitioning strategy is less influenced by the size of the intermediate data due to the higher mobile-edge network bandwidth (200 Mbps). Hence, the impact of the intermediate data size on inference latency is a crucial factor contributing to the observed performance advantage of the Mobile-Edge Partitioning strategy.

On the other hand, the Edge-Cloud Partitioning strategy achieves a speedup ranging from 1.03x to 1.26x when compared to the Mobile-Cloud Partitioning strategy, as shown in Figure 6 (yellow and green box-plots), along with small or large effect sizes (Table 12). These differences can be attributed to the faster computational capabilities of the Edge-Cloud tier compared to the Mobile-Cloud tier.

**The Edge Identity deployment strategy shows a 1.63x lower average median latency than the Mobile-Edge Partitioning strategy, which shows a 1.13x lower average median inference latency compared to the Mobile Identity Deployment strategy.**

Table 12: RQ4 Results of the Cliff’s Delta effect size between Mobile-Edge (ME), Edge-Cloud (EC), and Mobile-Cloud (MC) Partitioning strategies

$P_t \backslash P_x$	ME	EC	MC
ME	-	-L	-L
EC	-L	-	-L
MC	-L	-L	-

$P_f \backslash P_d$	ME	EC	MC
ME	-	-L	-L
EC	-L	-	-S
MC	-L	-L	-

<sup>1</sup>  $P_t$ ,  $P_x$ ,  $P_f$ ,  $P_d$  denotes Partitioning of the ResNet, ResNext, FCN, and DUC models, respectively.

The Edge Identity deployment strategy outperforms the Mobile-Edge Partitioning strategy, exhibiting a speedup ranging from 1.26x to 2.02x, as shown in Figure 6 (pink and dark blue boxplots), along with large effect sizes (Table 13). One possible explanation for this behavior is tier heterogeneity. In the Mobile-Edge deployment scenario, where distributed inference of partitioned models takes place, the tiers involved possess varying computation capabilities. Consequently, the processing speeds may vary, with slower tiers (such as mobile) impacting the overall inference latency. This suggests that the use of a Partition model may not be necessary for scenarios where a monolithic deployment tier such as edge is sufficiently capable of handling the computational load of the entire model.

In turn, the Mobile-Edge Partitioning strategy for all subjects (except DUC) achieves a speedup ranging from 1.11x to 1.26x compared to the Mobile Identity Deployment strategy, as shown in Figure 6 (dark blue and red boxplots), along with medium to large effect sizes (Table 13). Given that the Mobile tier in our study has the lowest computational resources compared to the more powerful Edge tier, offloading half of the computational load to the Edge tier alleviates the burden on the Mobile tier, resulting in reduced inference latency. These findings suggest that deploying partitioned models across resource-constrained tiers (i.e., Mobile and Edge) is more effective than deploying the entire model solely on the Mobile tier, due to the distribution of computational load during inference. For the DUC subject, the Mobile-Edge Partitioning strategy shows a 1.05x lower median inference latency than the Mobile Identity deployment strategy, with a large effect size. This is possible because of the large intermediate data size (781.25Mb) of the DUC model during distributed inference, which led to transmission overhead, even across the high mobile-edge network bandwidth of 200 Mbps, leading to a slower latency than the mobile tier.

**For ResNet/ResNext subjects, the Mobile-Edge, Edge-Cloud, and Mobile-Cloud strategies show 2.85x, 1.65, and 1.36 lower average median latency, respectively compared to the Cloud Identity deployment strategy. In contrast, in the case of FCN/DUC subjects, they show a 3.84x, 49.98x, and 52.14x higher average median inference latency.**

For ResNet/ResNext subjects, the Mobile-Edge, Edge-Cloud, and Mobile-Cloud Partitioning strategies achieve a speedup of 2.18x to 3.52x, 1.58x to 1.73x, and 1.25x to 1.48x, respectively, compared to the Cloud Identity Deployment strategy, as illustrated in Figure 6, along with medium to large effect sizes (Table 13). The lower intermediate data size (6.12 Mb) in comparison to the input data size (8 to 60 Mb) of these two subjects speeds up their transmission across the MEC tiers for the 3 multi-tier partitioning strategies. It suggests that Partitioning strategies can be a better alternative than cloud deployment for subjects having intermediate data sizes lower than the input data.

For FCN/DUC subjects, the Mobile-Edge, Edge-Cloud, and Mobile-Cloud Partitioning strategies exhibit 1.67x to 6.01x, 40.38x to 59.59x, and 41.68x to 62.60x higher median inference latency, respectively than the Cloud Identity deployment strategy, with large effect sizes (Table 13). For DUC, the intermediate data size (781.25 Mb) is much higher in comparison to the input data size (19-22 Mb) which led to its transmission overhead across both the Mobile-Edge (200 Mbps) and Edge-Cloud (1 Mbps) networks for the 3 Multi-tier Partitioning strategies. Conversely, for FCN, the intermediate data size varies between 118.12 Mb to 200 Mb, which is still much higher than their input data size (2-5 Mb), leading to transmission overhead. This is especially the case for the Edge-Cloud and Mobile-Cloud Partitioning strategies, which require transmission across the constrained Edge-Cloud network (1 Mbps). For the same subject, the slower latency of Mobile-Edge partitioning than of Cloud deployment is majorly due to the computational advantage of the Cloud compared to the Mobile-Edge tier. This suggests that cloud deployment can be a better alternative than Partitioning strategies for subjects having input data sizes smaller than the intermediate data. Moreover, for the FCN subject, which has the smallest input data

sizes among the four subjects, its Cloud Identity deployment strategy also shows faster latency than its Mobile/Edge Identity deployment strategies, as explained in RQ1 findings (Section 5.1).

**The Edge Early Exit/Quantized deployment strategy shows 1.96x/2.41x lower average median latency than the Mobile-Edge Partitioning strategy at a medium/small accuracy loss.**

The Edge Early Exit/Quantized deployment strategy shows lower median inference latency than the Mobile-Edge Partitioning strategy, ranging from 1.67x to 2.35x/ 1.87x to 2.44 across the four subjects, as shown in Figure 5 (blue, orange, green box-plots), along with large effect sizes (Table 8). In terms of accuracy, the Early Exit and Quantized operators show medium (2.53% to 11.56%) and small (0.05% to 0.38%) accuracy loss relative to Identity (or Partition) models as stated in RQ2 and RQ3 findings. This indicates that the Quantized and Early Exit operators at the Edge tier are a better alternative than the Partitioning operator at the Mobile-Edge tier in scenarios where sacrificing a small to medium level of accuracy may be acceptable to achieve faster latency.

Table 13: RQ4 Results of the Cliff's Delta effect size between Multi-tier (Mobile-Edge [ME], Edge-Cloud [EC], Mobile-Cloud [MC]) Partitioning Strategies and Single-tier (Mobile [M], Edge [E], Cloud [C]) Monolithic strategies.

$P_t \setminus I_t$	M	E	C
ME	-M	L	-L
EC	L	L	-L
MC	L	L	-M

$P_x \setminus I_x$	M	E	C
ME	-L	L	-L
EC	L	L	-L
MC	L	L	-L

$P_f \setminus I_f$	M	E	C
ME	-L	L	L
EC	L	L	L
MC	L	L	L

$P_d \setminus I_d$	M	E	C
ME	L	L	L
EC	L	L	L
MC	L	L	L

<sup>1</sup>  $P_t$ ,  $P_x$ ,  $P_f$ ,  $P_d$  denotes Partitioning of the ResNet, ResNext, FCN, and DUC subjects, respectively.

<sup>2</sup>  $I_t$ ,  $I_x$ ,  $I_f$ ,  $I_d$  denotes Identity versions of ResNet, ResNext, FCN, and DUC subjects, respectively.

#### Summary of Research Question 4

The Edge Identity/Early Exit/Quantized Deployment strategy shows faster latency (1.63x/1.96x/2.41x) at no/medium/small accuracy loss than the ME Partitioning strategy, which exhibits faster latency (1.13x) compared to the Mobile Identity Deployment strategy (1.13x), EC/MC Partitioning strategy (9.37x/9.86x), and Cloud Identity Deployment strategy (2.85x for ResNet/ResNext) in deployment scenarios where factors like input/intermediate data size and computational/network resources play a crucial role.

In scenarios where the subjects have smaller input data sizes (i.e., FCN) such that their transmission across the bandwidth-constrained cloud tier is not a major concern, their monolithic Cloud Identity deployment is much more effective than their Multi-tier Partitioning strategies and Edge/Mobile Identity Deployment strategies.

## 5.5 What is the performance impact of Hybrid operators within and across the tiers of the Edge AI Environment? (RQ5)

### 5.5.1 Quantitative Analysis of Quantized Early Exit (QE) operator on Monolithic Deployment tiers

**In Mobile, for 2 subjects (FCN/DUC), the QE models show 1.45x, 1.13x, and 1.35x lower average median inference latency than the Identity, Quantized, and Early Exit models, respectively. In Edge, for all subjects, the QE models show 1.75x, 1.17x, and 1.45 lower**

**average median inference latency than the Identity, Quantized, and Early Exit models, respectively. In Cloud, the QE models show no significant difference from the Identity, Quantized, and Early Exit models for all subjects (except DUC).**

In the Mobile tier, for FCN and DUC, the QE models show 1.29x to 1.62x and 1.16x to 1.54x lower median inference latency than the Identity and Early Exit models, respectively (Figure 5) along with large effect sizes (Table 7). Conversely, for the ResNet/ResNext subject, the QE models show 1.07x lower/1.05x higher (small effect sizes) and 1.11x (negligible effect size)/1.33x (large effect size) higher median inference latency than the Identity and Early Exit models, respectively. Even though the QE models have 4.61x to 5.04x and 3.90 to 3.98x lower size than the Identity and Early Exit models respectively, still they show slower latency for ResNet, ResNext, or both during mobile deployment, which indicates that these two subjects' Quantization Operations are costly in lower Memory/CPU environments, as mentioned in RQ2 findings (Section 5.2). Moreover, the QE models show 1.09x to 1.28x lower median inference latency than the Quantized models across the four subjects, with small to large effect sizes. This is possibly due to the addition of early exiting, which reduces computations during inference in comparison to a Quantized variant without any early exit similar to RQ3 findings (Section 5.3).

During Edge deployment, across the four subjects, the QE models exhibit 1.36x to 1.97x, 1.13x to 1.20x, 1.17x to 1.82x lower median inference latency than the Identity, Quantized, and Early Exit models, respectively, as depicted in Figure 5, with large effect sizes (Table 8). This suggests that the QE models exhibit greater robustness on the edge tier in comparison to the mobile tier. The higher computational resource on the edge tier is likely a contributing factor to this outcome.

According to the Conover test, the null hypothesis that there is no significant difference between QE and Identity, QE and Quantized, QE and Early Exit models in the Cloud cannot be rejected for three subjects (i.e., ResNet, ResNext, FCN), indicating their similar or equivalent latency performance in the cloud. Due to the powerful computing resources of the cloud, the impact of the QE models is not significant compared to the Identity, Quantized, and Early Exit models. However, for the DUC subject, the null hypothesis was rejected with p-values of  $8.9e^{-221}$ ,  $6.8e^{-10}$  and  $1.5e^{-196}$  ( $\alpha = 0.05$ ) for QE vs Identity, QE vs Quantized, and QE vs Early Exit comparison, respectively, indicating significant inference latency difference between them. For the DUC subject, the QE models show slower latency than the Identity and Early Exit models with large effect sizes (Table 9). We believe that this is due to the lowest percentage of graphical nodes processed with the CUDA Execution Provider for DUC during Cloud deployment, similar to the reasoning explained briefly for the RQ2 results (see first finding in Section 5.2). For the same subject, the QE model shows faster latency than the Quantized model, but with a small effect size, possibly due to the minor influence of early exiting.

**The QE models show a medium drop in accuracy relative to Identity, Quantized, and Early Exit models.**

In Table 6, an accuracy drop of 2.62% to 12.41%, 2.56% to 12.02%, 0.09% to 1.66% is observed when comparing the performance of the QE models with the Identity, Quantized, and Early Exit models, respectively. These accuracy differences are statistically significant (Wilcoxon Test:  $p\text{-value} = 7.6e^{-6}$ ,  $\alpha = 0.0125$ ), with medium effect sizes. For applications prioritizing real-time inference in the Edge tier and willing to accept a medium decrease in accuracy compared to the Identity, Quantized, and Early Exit models, the utilization of a hybrid (Quantized + Early Exit) model may be a suitable choice.

**When comparing QE across the three Monolithic Deployment tiers, the QE models during Edge deployment show 2.63x and 3.89x lower average median inference latency than their deployment in Mobile and Cloud tiers, respectively.**

The QE models in the Edge tier demonstrate 2.03x to 2.90x lower median inference latency compared to the Mobile tier as shown in Figure 5 (red box plots), with large effect sizes (Table 14) due to Edge's higher computational resources. Among the Edge and Cloud tiers, the QE model's median inference latency under-performs by 1.77x to 7.69x during Cloud deployment for three subjects (i.e., ResNet, ResNext, DUC), along with large effect size (Table 14). This is due to the higher impact of large input data sizes of these subjects on the transmission across the restricted edge-cloud network during cloud deployment. Conversely, for the FCN subject, the QE model exhibits 1.93x lower median inference latency in the Cloud tier compared to the Edge tier, with a large effect size (Table 14). Similarly, this is due to FCN's small input data sizes, leading to lower impact on data transmission across the constrained edge-cloud network during cloud deployment. The reasoning behind these findings is similar to and explained briefly in the RQ1 findings (Section 5.1).

Table 14: RQ5 Results of the Cliff's Delta effect size between Mobile (M), Edge (E), and Cloud (C) Deployment for QE models

$QE_x$	$QE_t$	M	E	C
M	-	L	-L	
E	L	-	-L	
C	-L	-L	-	

$QE_d$	$QE_f$	M	E	C
M	-	L	L	
E	L	-	L	
C	L	-L	-	

<sup>1</sup>  $QE_t$ ,  $QE_x$ ,  $QE_f$ ,  $QE_d$  denotes Quantized Early Exit versions of ResNet, ResNext, FCN, and DUC, respectively.

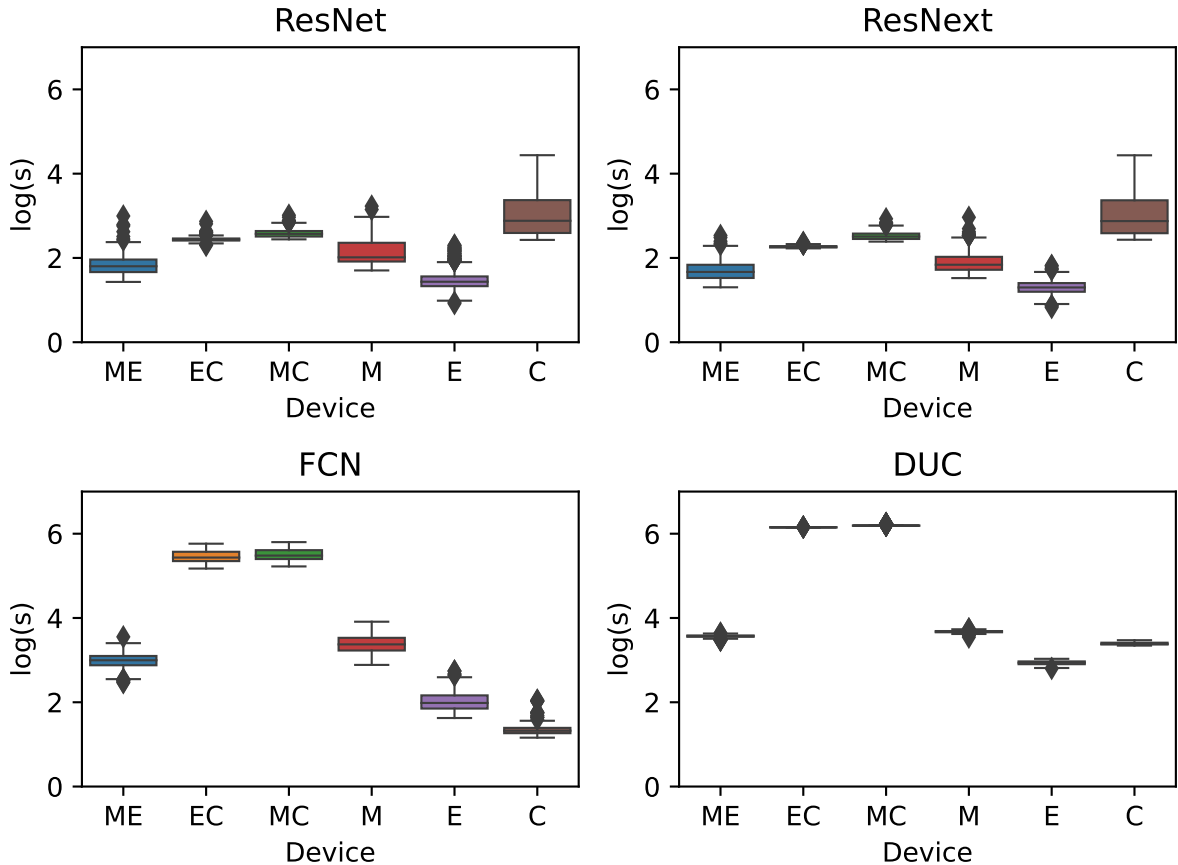


Fig. 7: Box plots of the Inference Latency measure for Multi-tier QEP strategies and Monolithic QE deployment strategies involving 6 Deployment tiers (i.e., Mobile-Edge[ME], Edge-Cloud[EC], Mobile-Cloud[MC], Mobile[M], Edge[E], Cloud[C])

### 5.5.2 Quantitative Analysis of QEP Strategy and its Comparison with Monolithic Deployment Strategies

Across the three Multi-tier QEP strategies, the Mobile-Edge QEP strategy shows an 8.51x and 9.04x lower average median inference latency than Edge-Cloud and Mobile-Cloud QEP strategies, respectively.

The Mobile-Edge QEP strategy accounts for 1.73x to 15.65x and 2.21x to 16.20x lower median inference latency than the Edge-Cloud and Mobile-Cloud QEP strategies, respectively (Figure 7), with large effect size (Table 15). On the other hand, the Edge-Cloud QEP strategy shows 1.04x to 1.28x lower median inference latency than the Mobile-Cloud QEP strategy as shown in Figure 7, along with small or large effect sizes (Table 15). This is due to similar reasons as explained in the RQ4 results (see first finding in Section 5.4).

Table 15: RQ5 Results of the Cliff’s Delta effect size between Mobile-Edge (ME), Edge-Cloud (EC), and Mobile-Cloud (MC) QEP Strategies

$QEP_x \backslash QEP_t$	ME	EC	MC
ME	-	-L	-L
EC	-L	-	-L
MC	-L	-L	-

$QEP_d \backslash QEP_f$	ME	EC	MC
ME	-	-L	-L
EC	-L	-	-S
MC	-L	-L	-

<sup>1</sup>  $QEP_t$ ,  $QEP_x$ ,  $QEP_f$ ,  $QEP_d$  denotes Quantized Early Exit Partition versions of ResNet, ResNext, FCN, and DUC subjects

**The Edge QE deployment strategy shows 2.03x lower average median inference latency than the Mobile-Edge QEP strategy, which shows 1.29x lower average median inference latency than the Mobile QE deployment strategy.**

The Edge QE strategy outperforms the Mobile-Edge QEP strategy with large effect sizes (Table 16), exhibiting a speedup ranging from 1.85x to 1.94x, as shown in Figure 7. In turn, the Mobile-Edge QEP strategy shows 1.09x to 1.47x lower median inference latency than the Mobile QE strategy (large effect sizes) as shown in Figure 7 and Table 16. In general, this suggests that distributed model deployment across mobile and edge tiers can be an optimal choice compared to monolithic model deployment in a resource-constrained environment (such as mobile) when faster inference is a concern at no accuracy loss. This is due to similar reasons provided in RQ4 results (see second finding in Section 5.4).

**For ResNet/ResNext, the Mobile-Edge, Edge-Cloud, and Mobile-Cloud QEP strategies show 3.41x, 1.82x, and 1.44x lower average median latency, respectively than the Cloud QE deployment strategy. In contrast, in the case of FCN/DUC, they show 2.39x, 36.92x, and 38.28x higher average median inference latency.**

For ResNet and ResNext, the Mobile-Edge, Edge-Cloud, and Mobile-Cloud QEP strategies demonstrate a lower median inference latency of 3.12x to 3.70x, 1.80x to 1.84x, and 1.40x to 1.48x, respectively than the cloud QE strategy as shown in Figure 7), along with large effect sizes (Table 16). Conversely, for FCN and DUC, the same strategies exhibit a 1.04x to 3.74x, 15.28x to 58.57x, and 15.91x to 60.65x higher median inference latency, along with medium to large effect sizes (Table 16). A possible explanation for these results is similar to the RQ4 results (see third finding in Section 5.4). Moreover, for the FCN subject, which has the lowest input data sizes among the four subjects, its Cloud QE deployment strategy also shows faster latency than its Mobile/Edge QE deployment strategies, as explained previously in RQ5 findings (Section 5.5).

**The Edge Identity/Quantized/Early Exit deployment strategy shows 1.17x/1.72x/1.42x lower average median latency at medium accuracy gain when compared with Mobile-Edge QEP strategy, which shows 1.39x lower average median latency than the Mobile-Edge Partitioning strategy at medium accuracy loss.**

The Edge Identity/Quantized/Early Exit deployment strategies show 1x to 1.35x/ 1.61x to 1.88x/ 1.24x to 1.59x lower median inference latency than the Mobile-Edge QEP strategy across the four subjects, as shown in Figure 5 (blue, orange, green, red box-plots), along with medium to large effect sizes (Table 8). In terms of accuracy, the Identity, Quantized, and Early Exit models show medium accuracy gain (i.e., 2.62% to 12.41%, 2.56% to 12.02%, 0.09% to 1.66%) relative to QE (or QEP) models as stated previously in the second finding of RQ5 (Section 5.5.1). This indicates that the non-hybrid operators (Identity, Quantized, and Early Exit) at the Edge tier are a better alternative than the hybrid QEP operator at the Mobile-Edge tier in scenarios where maximizing both latency and accuracy are of utmost importance. Moreover, the Mobile-Edge QEP strategy shows 1.04x to 1.60x lower median inference latency with large effect sizes (Table 8) than the Mobile-Edge Partitioning strategy but at a cost of medium accuracy loss (2.62% to 12.41%).

Table 16: RQ5 Results of the Cliff's Delta effect size between Multi-tier (Mobile-Edge [ME], Edge-Cloud [EC], Mobile-Cloud [MC]) QEP Strategies and Single-tier (Mobile [M], Edge [E], Cloud [C]) QE strategies.

$QEP_t$	$QE_t$			$QEP_x$	$QE_x$		
	M	E	C		M	E	C
ME	-L	L	-L	ME	-L	L	-L
EC	M	L	-L	EC	L	L	-L
MC	L	L	-L	MC	L	L	-L

$QEP_f$	$QE_f$			$QEP_d$	$QE_d$		
	M	E	C		M	E	C
ME	-L	L	L	ME	-L	L	M
EC	L	L	L	EC	L	L	L
MC	L	L	L	MC	L	L	L

<sup>1</sup>  $QEP_t$ ,  $QEP_x$ ,  $QEP_f$ ,  $QEP_d$  denotes Quantized Early Exit Partition of ResNet, ResNext, FCN, and DUC subjects, respectively.

<sup>2</sup>  $QE_t$ ,  $QE_x$ ,  $QE_f$ ,  $QE_d$  denotes Quantized Early Exit versions of ResNet, ResNext, FCN, and DUC subjects, respectively.

### Summary of Research Question 5

The QE operator shows 1.75x/1.17x/1.45 faster latency than the Identity/Quantized/Early Exit operator in the Edge tier at medium accuracy loss (up to 12.41%/12.02%/1.66%). The Edge deployment of hybrid (QE) and non-hybrid (Identity/Quantized/Early Exit) operators show 2.03x and 1.17x/1.72x/1.42x faster latency at no accuracy loss and medium (up to 12.41%/12.02%/1.66%) accuracy gain, respectively than the ME QEP strategy, which shows faster latency than the ME Partitioning strategy (1.39x at medium accuracy loss), EC/MC QEP (8.51x/9.04x), Mobile QE (1.29x), & Cloud QE (3.41x for ResNet/ResNext) strategies for scenarios influenced by input/intermediate data size of the subjects and computational/bandwidth resources of the MEC tiers.

In scenarios where the subjects have smaller input data sizes (i.e., FCN) such that their transmission across the bandwidth-constrained cloud tier is not a major concern, their monolithic Cloud QE deployment is much more effective than their Multi-tier QEP strategies and Edge/Mobile QE Deployment strategies.

## 6 Discussion

Among the three monolithic deployment tiers, the edge tier consistently demonstrates significantly faster inference latency performance for each operator examined in the respective research questions (i.e., Identity operator in RQ1, Quantized operator in RQ2, Early Exit operator in RQ3, and Quantized Early Exit operator in RQ5). This outcome underscores the significance of deployment operators involved in the edge tier compared to mobile and cloud tiers when facing computational limitations, network bandwidth constraints, and large input data transmission. The edge tier's closer proximity to the mobile and higher computational resources allow faster processing and reduced transmission latency, resulting in improved inference latency performance.

In the Cloud tier, the comparisons between the Quantized operator and the identity operator (RQ2) as well as between the QE operator and the Early Exit/Identity operator (RQ5) do not show any significant difference (Conover Test) for any subjects, except DUC. The main challenge is the inability of the CUDA execution provider in the ONNX Runtime Inference Engine to fully support the CUDA kernels used for the quantized graphical nodes during cloud deployment. The unavailability of the CUDA kernel for the nodes of the Quantized/QE models leads to their execution being run on the CPU instead. This introduces some overhead due to the lower processing power of the CPU in comparison to the CUDA. Future research efforts can delve into solutions for optimizing the quantization in a GPU-based cloud

environment. One solution might be to modify the model structure and its operations to avoid nodes that lack CUDA kernels. Techniques such as operator fusion, where multiple operations are combined into a single operation, could be beneficial. Another solution could be to develop custom CUDA kernels for the nodes of the Quantized/QE models that currently lack them. This would require a deep understanding of both CUDA programming and the specific operations performed by the incompatible nodes. Utilizing other GPU-specific execution providers like TensorRT instead of CUDA was not considered due to the reasoning provided in Section 7.

On Cloud, the comparisons between the Early Exit and Identity operator (RQ3) as well as between the QE and Quantized operator (RQ5) show no significant difference for the Resnet/ResNext/FCN subject and even if the difference is significant (in the case of DUC) based on the post-hoc test, the effect size remains negligible to small. This suggests that the advantages provided by these specialized operators in terms of speedup may be less pronounced in cloud deployments, where computational resources are typically more abundant. In the above scenarios, the use of the identity operator alone may be sufficient, and incorporating specialized operators like quantization, early exit or their combinations may not yield significant benefits in terms of improving latency.

Among the three multi-deployment tiers (Mobile-Edge, Edge-Cloud, and Mobile-Cloud), the Mobile-Edge tier consistently exhibits faster latency performance for each operator examined in their respective research questions (i.e., Partition operator in RQ4 and QEP operator in RQ5). The key contributing factor to the Mobile-Edge tier’s superiority is the higher network bandwidth it offers, which facilitates faster transmission of intermediate outputs during distributed inference. The Mobile-Edge distributed inference consistently shows faster latency performance than stand-alone mobile inference for Identity models in RQ4 and QE models in RQ5 due to the computational load distribution. The Partitioning of Identity/QE models should ideally not influence the accuracy drops as it aims to divide the model into smaller components without altering the computations or operations performed, as stated in [68]. In other words, the computations within the partitioned models are consistent with the original model’s computations. The models considered in previous studies for CV tasks are relatively small (i.e, lower size) and less complex, which potentially resulted in findings that Mobile deployment is a better alternative than Mobile-Edge Partitioning (Kang et al [45]). However, in our study, where complex models are considered as the subjects, partitioning across the Mobile and Edge is a better alternative than doing the local computing of the whole model on a resource-constrained mobile tier, especially when faster latency is a concern at no accuracy loss.

In previous studies (Table 1), the resolution of input data size is relatively small as they are validated only on small-scale datasets such as MNIST and CIFAR datasets, and/or they did not explicitly analyze the impact of high-resolution images (from Image Net, COCO, and CityScapes datasets) on the end-to-end latency evaluation of operators in MEC tiers. Eshratifar et al. [20] suggest that using either local computing only or cloud computing only is not an optimal solution in terms of inference latency in comparison to model partitioning. However, the key issue is that they considered a single image for the end-to-end sequential inference across the Mobile-Cloud tier, without exploring the variation of input data sizes. In our study, the impact of multiple and varying image sizes on end-to-end latency was explored, which resulted in more generalized findings. Based on our results, the subjects having low-resolution images (such as FCN) may favor network-constrained Cloud deployment in comparison to Multi-tier partitioning strategies and Mobile/Edge deployment, as the impact on transmission overhead for smaller-sized images reduces and the cloud as usual has better computational capabilities. For subjects (i.e., ResNet, ResNext, DUC) having large-sized image samples, Edge deployment is a better alternative than Multi-tier partitioning strategies and Mobile/Cloud deployment.

Prior work [20, 43, 45, 53, 116, 82, 16, 113, 74, 56, 39] explores factors such as the computational load, network cost, energy consumption, and/or privacy risk for each of the DNN partitioning points in an Edge AI setup to dynamically decide the optimal partition point, and stated that the model partitioning operator achieves significant latency speedup i.e., latency reduction compared to traditional Mobile and/or Cloud deployment, similar to our findings, i.e., Mobile-Edge distributed inference of Partitioned/QEP models is a better alternative than resource-constrained Mobile deployment of Identity/QE models. When comparing the Multi-tier distributed strategies of Partitioned/QEP models with the Cloud deployment of Identity/QE models in RQ4/RQ5, the intermediate data size and input data size play a crucial role. For FCN and DUC, the intermediate data size of their Partitioned/QEP variants is larger than their input data sizes, correlating with faster cloud inference than distributed inference. Conversely, for ResNet and ResNext, the intermediate data size of their Partitioned/QEP variants is smaller than their input data

sizes, correlating with faster-distributed inference than cloud inference. Different partition points (specific graphical node connection(s) within the neural network architecture where the model is divided or split into two sub-models) might have different intermediate data sizes and their impact on the latency might vary. However, in our study, we limited our research to a single partition point, as the goal was to create equal-size partition models (which require a single partition point). Although our partitioning approach simply and fairly splits the models statically into two sub-models to have equal sizes, one running at the mobile/edge, and the other one in the edge/cloud, it requires manual analysis of the ONNX computational graphs of the subject models, which varies in terms of graph complexity and architecture design. In terms of subject models considered for model partitioning, previous studies performed their experiments on lightweight CV models, which are less complex and less accurate than the heavy-weight state-of-the-art CV models considered in our study.

In previous studies performing early exiting [19, 48, 60, 84, 95, 99, 100, 101, 104, 109, 111, 112, 116, 121, 59, 67, 110, 106], there is a trade-off between accuracy and latency. This trade-off in early exiting comes from the fact that exiting earlier in the network can reduce latency but may also result in less accurate predictions. This is because the early layers in a DNN generally extract low-level features, while the later layers extract high-level features that are more task-specific. Therefore, an early exit at early layers might miss important high-level features, leading to a decrease in accuracy. On the other hand, waiting for the network to reach the later layers can increase the accuracy but also increase the latency. In our case, the early exiting was performed in the later stage of the models, which showed faster latency than the original model but at a medium accuracy loss. One of the reasons for this significant accuracy loss is that the early exiting approach in our study is based on the condition of manually short-circuiting identically structured sub-graphs on pre-trained models. This means that the early exits are added in a black-box manner on pre-trained models without retraining them, which contributes to this accuracy loss. Previous studies perform DNN early exiting that requires training of the models, which results in better accuracy performance for early exiting even in earlier stages of the model.

As stated in previous studies [53, 4, 5, 9, 23, 25, 36, 51, 71, 77, 94, 26, 41, 119, 55], the Quantization operator in our study also shows a small (not significant) accuracy drop in comparison to the original model. In addition to that, we also compared the Quantization operator's performance with other operators like Early Exit and Quantized Early Exit operators, concluding that during edge deployment, the Quantization can be used in scenarios where the least accuracy drop is of utmost importance w.r.t the original model, at the benefit of faster latency than Early Exit and the cost of slower latency than Quantized Early Exit operators.

In terms of effort, the use of an automated tool like Intel Neural Compressor for applying the quantization operator suggests a streamlined and automated process for Edge AI model deployment. This implies that, right now, the quantization process can be performed without manual effort and intervention, as a tool automates the necessary modifications to achieve model quantization. Yet, while applying quantization to models from the ONNX Model ZOO and torchvision.models subpackage, we observed that some of the models contain unsupported ONNX operations that are not listed in the supported ONNX schema<sup>7</sup>, due to which the model may not be feasible for quantization without additional modifications or workarounds. For instance, while converting models from Pytorch to ONNX format, the converted ONNX models can include custom layers or operations that are specific to the Pytorch framework and hence lack quantization support in ONNX.

On the other hand, applying the Early Exit operator on Identity/Quantized models and the Partitioning operator on Identity/Quantized Early Exit models currently requires manual analysis of the ONNX computational graphs using the Netron Visualizer tool <sup>8</sup> and manual modifications of the neural network using ONNX Python APIs. We observed that performing these deployment operators on ONNX models from other classes (e.g., textual inference task), was not always feasible due to the complex architecture of the ONNX computational graph. The complex architecture of such models includes various layers, connections, and branching structures that can make it difficult to identify suitable partition points or early exit points. In such cases, applying these operators might require significant manual analysis and modifications of the model's computational graph, which can be time-consuming and error-prone.

The provided empirical results for these operators on the 4 Image Classification and Segmentation subjects give valuable insights into the speed and performance of operators across and within tiers under

---

<sup>7</sup> <https://github.com/onnx/onnx/blob/main/docs/Operators.md>

<sup>8</sup> <https://github.com/lutzroeder/netron>

various deployment scenarios, which could inspire work related to the automation of these operators for future studies in the field of MLOps. Additionally, the empirical approach employed in our study, and the empirical results obtained, can be used as a foundation for developing recommendation systems for Edge AI operators.

## 7 Threats to Validity

Below, we discuss threats to the study validity and the strategies we applied to mitigate these threats, based on literature guidelines [105].

*Construct Validity:* One possible threat is the mono-operation bias caused by having only one factor of network bandwidth, computational configuration (RAM/CPU), Early Exiting point, and Partitioning point. The mobile-edge network bandwidth of 200 Mbps and edge-cloud network bandwidth of 1 Mbps was used to simulate the close and distant proximity of mobile-edge and edge-cloud environment, respectively based on earlier work [78, 118, 96, 24, 2]. The computational simulations of MEC tiers are also based on previous studies [15, 17, 47, 87]. Variations in the network bandwidths and the computational resources can impact the end-to-end inference latency for the deployment strategies. In a previous study [86], Docker containers running on a server are used to simulate several resource-constrained tiers in a realistic IOT framework. This is similar to what we did for simulating the resource-constrained tiers (i.e., mobile and edge) in our study.

In real-world scenarios, variations in hardware across different edge/mobile devices are possible and may impact the generalizability of our simulated setup. Simulating the impact of multiple factors is very costly as it involves running numerous experiments, each taking considerable time to complete and requiring significant computational resources. While we acknowledge the importance of diverse deployment scenarios having different computational/network configurations of MEC tiers, the specific experimental setup was chosen strategically to provide a focused exploration of a typical Edge AI environment having a resource-scarce mobile device, an Edge device's closer proximity, and higher computational capacity w.r.t Mobile device, together with a resource-abundant cloud device with network constraints.

In our study, we focus on Early Exit at a single stage of the neural network. However, it is important to note that early exiting at multiple stages of the network can result in varying accuracy performance. Early exiting at a later stage may yield higher accuracy but slower inference due to more processing required before making predictions. On the other hand, the early exit at an earlier stage may provide faster inference but with lower accuracy since the predictions are made based on less processed information. The detailed explanation for selecting the early exit criteria is mentioned in the RQ3 approach (Section 4.5.3), and requires manual inspection of the subjects' ONNX computational graphs. Similarly, for partitioning, we considered the partition point that leads to equal-sized sub-models for effective and fair load distribution across the tiers involved in distributed inference. Our study acknowledges the limitations associated with this simplified model partitioning approach. We recognize that real-world scenarios often entail more complex partitioning strategies as mentioned in related work (Section 1), especially when dealing with intricate model architectures, such as partitioning at each of the layers of DNN models and analyzing their impact on various factors like computational, transmission, and/or energy cost.

In our study, the decision to adopt a simplified approach stems from the need for a fair evaluation of the subject models. By manually inspecting the ONNX computational graphs of the DNN models, we aim to establish a baseline understanding of the challenges and dynamics involved in equal-size partitioning of the DNN models with varying and complex architectures, specifically in the ONNX framework. The manual insights of the computational graphs of the subjects will assist MLOps Engineers in understanding the factors involved in constructing an automated tool to dynamically decide the optimal partition point to achieve equal-size sub-models for subjects with varying architectures. This approach might have an adverse impact on the transmission of intermediate data during distributed inference across the MEC tiers, as shown for two of the subjects (FCN, DUC) in our study. Different partition points may have different intermediate data sizes which can yield latency benefits during distributed inference across MEC tiers in scenarios where the intermediate data size is lower than the input data size, as shown (ResNet and ResNext) in our study.

*Conclusion Validity* We considered the Static Post-Training Quantization (PTQ) approach over the Dynamic PTQ approach due to its faster inference capabilities. Dynamic PTQ requires additional computational overhead during inference because of the dynamic recalibration process in which the model's

weights and activations are recalibrated based on the input data’s statistics during inference. On the other hand, Static PTQ involves quantizing the model’s weights and activations only once during the model conversion phase, without the need for recalibration during inference. Since the quantization parameters are precomputed and do not change during inference, the quantization process is much simpler and requires fewer computations during inference.

*Internal Validity:* The risk of how history might affect the inference latency results of the deployment strategies is reduced by performing all measurements in the same Edge AI environment, using the same infrastructure. To maintain uniformity and minimize variations, we developed automated scripts to execute the inference experiments for the deployment strategies sequentially, one after another. Before starting an inference experiment, we took the necessary step of restarting the Docker containers to eliminate any potential residual effects from the previous inference experiment. In our experiments, we considered sequential inference (i.e., 1 request at a time) instead of parallel inference (i.e., multiple requests at a time). Sequential inference allows us to efficiently utilize the available resources for each deployment strategy, ensuring a more accurate representation of their true inference latency performance [117], similar to how micro-benchmarks operate. The goal of our study was not load testing [44], where the focus would be on measuring the system’s ability to handle multiple concurrent inference requests. Performing parallel inference may lead to resource contention, which could obscure the true impact of deployment strategies. Similarly, the Scalability aspects, such as the impact of increasing the number or complexity of models deployed simultaneously in a real-world setting, are not explored, as they are outside the scope of this study, since our micro-benchmarks will not focus on system-level measurements.

It is worth mentioning that the ONNX Run-time Inference Engine may perform worse on the first input received than on subsequent inputs during inference experiments of deployment strategies, mainly because of a required warm-up inference. To remove such bias, we used a trial inference experiment. For each deployment strategy, a trial experiment of 100 inference runs is performed sequentially to reach a steady state of the cache, then the final inference experiment of 500 runs = 100 (input samples) x 5 (repetitions) is performed sequentially (and repeatedly) without any cool-down period between subsequent runs to simulate the scalability of each deployment strategy. Note that the relatively high standard deviation in the inference latency measure for each deployment strategy might have been caused by having 5 repetitions per sample run; this potential source of bias can be mitigated by increasing the number of such repetitions. In our study, it is costly to do this due to the computational and transmission overhead caused by factors like large model size and input/intermediate data transmission. The 100 input samples considered are selected based on a filter based on size to analyze the impact of input data on the total inference latency.

*External Validity:* The selection of the subjects might constitute another potential threat as it was performed manually. Thus, the selected set of subjects could not be regarded as an accurate representation of the whole population. The first iteration in this process consisted of choosing a set of subjects from the ONNX Zoo and PyTorch Models, initially aiming to have two representatives from each class (i.e., the inference task). However, we observed a lack of already trained models from some of the classes and what is more, most of the models were not feasible for Partitioning/Early Exiting due to the complex ONNX graph architectures, or for Quantization due to some operations or layers in the ONNX graph architectures that may not have quantization support in the neural compressor tool. As a result of that, we ended up with a selection of four subject models, from the Computer Vision (CV) category. This threat is reduced by aiming to diversify the Inference tasks they performed (i.e., Image Classification and Image Segmentation).

The majority of the previous studies, as shown in Table 1, focus on CV tasks for the operators due to their major impact on various factors like computational load and data transmission during deployment in an Edge AI environment. Therefore, the choice of CV domain for subject models and datasets is quite common. However, we do acknowledge that different types of models (e.g., Natural Language Processing and Speech Recognition) may exhibit different behaviors in response to deployment strategies. In our study, we limited the scope of our study to three black box operators, i.e., Partition, Quantization, and Early Exiting, as these are most commonly used, which do limit the comprehensiveness of the studied operators. Overall, the selection of subjects (datasets/models) and deployment operators is one of the external threats concerning this study. This threat can be mitigated in the future by repeating the experiment on other domain-specific subjects (e.g. Natural Language Processing, Speech Recognition) and white-box operators (e.g., Quantization Aware Training, Weight Pruning, Knowledge distillation) as mentioned in Table 1.

The effectiveness and compatibility of the Intel Neural Compressor tool for quantization might vary for different models or frameworks (i.e., ONNX), affecting the reproducibility of the study in different environments (i.e., CPU, GPU). In our results, for some subjects like ResNet and ResNext, their Quantized and QE models show slower latency performance than Identity and Early Exit models in resource-constrained environments (i.e., mobile). Yet, for other subjects (like FCN and DUC), their Quantized and QE models show faster latency performance than Identity and Early Exit models in the same environment. Conversely, in high-resource environments (i.e., Edge), all subjects' Quantized and QE models show faster latency than the Identity and Early Exit models. This shows that for different subjects the compatibility of this tool (i.e., Intel Neural Compressor) for quantization might vary in terms of latency performance in computationally varying environments. Moreover, this tool might show different latency or accuracy behavior for models in different formats (such as Pytorch and Tensorflow). Moreover, the visual analysis of the computational graphs might vary with different models, frameworks, or visualization tools.

Among the GPU specific Execution providers (i.e., CUDA, TensorRT), we considered CUDA in a GPU-based environment (i.e., Cloud ) due to its inference benefits<sup>9</sup><sup>10</sup> compared to TensorRT. First, it is faster to initialize because it only evaluates small network building blocks during its exhaustive search. In particular, the CUDA Execution Provider uses the cuDNN inference library, which is based on granular operation blocks for neural networks. Moreover, CUDA is more versatile in handling inference tasks with varying sizes, is generally easier to use, and requires less setup. On the other hand, TensorRT evaluates the whole graph and collects all possible paths to execute the graph, which can take multiple minutes for large ONNX models. Second, TensorRT can allocate workspace memory for intermediate buffers inside the network, resulting in high memory usage. Lastly, when dealing with images of various sizes (like our study), TensorRT might be slower due to constantly recomputing the engine under a different size. Therefore, utilizing other GPU-specific execution providers like TensorRT might not be an optimal choice.

Instead of using actual devices, we used docker containers for simulating the hardware and network configurations of physical mobile, edge, and cloud devices to create real-time deployment scenarios. The Docker simulations allow flexibility by easily configuring the network/hardware settings. Setting up and maintaining actual devices can be expensive and require more experience, especially for simulating different configurations and deployment scenarios. Docker containers provide a cost-effective way to create virtual environments that closely mimic the behavior of real hardware without the need for additional physical resources. The latest versions of all the tools and packages were employed on the simulated devices in the experimental setup (Section 4). The generalization factor can be improved by replicating the experiment on different hardware and network configurations of the devices. In other words, Real-world deployment considerations, such as network variability, security implications, or dynamic edge environments should be considered for generalization.

In our study, we computed the inference accuracy performance independently on multiple representative deployment tiers (i.e., Mobile, Edge, Cloud) for four different types of accuracy-sensitive operators (i.e., Identity, Quantized, Early Exiting, and Quantized Early Exiting) to provide valuable insights into the model's generalizability across different hardware targets, specifically CPUs and GPUs. The ONNX models are designed to be hardware-agnostic and can be deployed on various hardware devices without significant modifications. This allows the models to achieve consistent accuracy performance across different deployment environments, as long as the hardware supports the necessary operations and computational capabilities.

We applied the operators to the subjects in ONNX format and performed the inference of the transformed models using the ONNX Runtime Engine due to optimized deployment performance benefits, as suggested by previous studies [80,34]. The feasibility of scripting black-box transformations using Python ONNX APIs was another reason for considering subject models in ONNX format, instead of other formats (like Pytorch and Tensorflow).

---

<sup>9</sup> <https://developer.nvidia.com/blog/end-to-end-ai-for-nvidia-based-pcs-cuda-and-tensorrt-execution-providers-in-onnx-runtime>

<sup>10</sup> <https://github.com/chaiNNer-org/chaiNNer/discussions/2437>

## 8 Conclusion

Deploying black-box models (deep neural networks) efficiently in an Edge AI setting introduces unique challenges for MLOps engineers and software practitioners. The black-box models require specific considerations for optimization in resource-constrained and network-constrained deployment scenarios. This paper aims to be an important stepping stone in the field of MLOps, in particular for the deployment of black-box models, to evaluate the benefits and trade-offs of Edge AI deployment strategies involving mappings of <operators, tiers>, by evaluating their performance in terms of quantitative metrics like Latency and Accuracy. While previous works focused on exploring and addressing individual operators (i.e., partitioning, early exiting, quantization), our study has systematically compared the individual operators and their unexplored combinations in Edge AI Environment using empirical data of 4 major computer vision subjects for testing the various deployment strategies.

The MLOps engineers could prefer Mobile-Edge distributed inference when faster latency is a concern in deployment scenarios where the mobile tier has strict resource (CPU/RAM) requirements. For models with smaller input data size requirements, their deployment at the Cloud tier with limited network bandwidth capacity can also be a better alternative than Model Partitioning across MEC tiers and Mobile/Edge deployment. For models with large input data size requirements, Edge deployment can be a priority over Model Partitioning and Mobile/Cloud deployment in scenarios where the Edge has higher computational/network capabilities than the Mobile/Cloud. Among the studied operators, the Edge deployment of the Quantize Early Exit operator could be the preferred choice over the Edge deployment of the Early Exit/Quantize operator and Mobile-Edge deployment of the Partition operator when faster latency is a requirement at medium accuracy loss. In contrast, for MLOps engineers having requirements of the minimal accuracy loss w.r.t the original model, the Edge deployment of the Quantize operator could be the preferred choice at the benefit of faster latency over the Edge/Mobile-Edge deployment of the Early Exit/Partition operator and the cost of slower latency over the Edge deployment of Quantize Early Exit operator. In future work, we plan to further investigate the impact of white box operators for deployment in an Edge AI environment.

## 9 Conflict of Interests

All authors declare that they have no conflicts of interest.

## 10 Data Availability Statement

The models generated and analyzed during the current study are available from the corresponding author upon reasonable request.

## References

1. ALZUBAIDI, L., ZHANG, J., HUMAIDI, A. J., AL-DUJAILI, A., DUAN, Y., AL-SHAMMA, O., SANTAMARÍA, J., FADHEL, M. A., AL-AMIDIE, M., AND FARHAN, L. Review of deep learning: Concepts, cnn architectures, challenges, applications, future directions. *Journal of big Data* 8 (2021), 1–74.
2. ANDRÉS RAMIRO, C., FIANDRINO, C., BLANCO PIZARRO, A., JIMÉNEZ MATEO, P., LUDANT, N., AND WIDMER, J. open-leon: An end-to-end emulator from the edge data center to the mobile users. In *Proceedings of the 12th International Workshop on Wireless Network Testbeds, Experimental Evaluation & Characterization* (2018), pp. 19–27.
3. ASSINE, J. S., VALLE, E., ET AL. Single-training collaborative object detectors adaptive to bandwidth and computation. *arXiv preprint arXiv:2105.00591* (2021).
4. BANNER, R., NAHSHAN, Y., AND SOUDRY, D. Post training 4-bit quantization of convolutional networks for rapid-deployment. *Advances in Neural Information Processing Systems* 32 (2019).
5. CAI, Y., YAO, Z., DONG, Z., GHOLAMI, A., MAHONEY, M. W., AND KEUTZER, K. Zeroq: A novel zero shot quantization framework. In *Proceedings of the IEEE/CVF Conference on Computer Vision and Pattern Recognition* (2020), pp. 13169–13178.
6. CHIANG, C.-H., LIU, P., WANG, D.-W., HONG, D.-Y., AND WU, J.-J. Optimal branch location for cost-effective inference on branchynet. In *2021 IEEE International Conference on Big Data (Big Data)* (2021), IEEE, pp. 5071–5080.
7. CHOI, H., AND BAJIĆ, I. V. Deep feature compression for collaborative object detection. In *2018 25th IEEE International Conference on Image Processing (ICIP)* (2018), IEEE, pp. 3743–3747.

8. CHOI, H., COHEN, R. A., AND BAJIĆ, I. V. Back-and-forth prediction for deep tensor compression. In *ICASSP 2020-2020 IEEE International Conference on Acoustics, Speech and Signal Processing (ICASSP)* (2020), IEEE, pp. 4467–4471.
9. CHOUKROUN, Y., KRAVCHIK, E., YANG, F., AND KISILEV, P. Low-bit quantization of neural networks for efficient inference. In *2019 IEEE/CVF International Conference on Computer Vision Workshop (ICCVW)* (2019), IEEE, pp. 3009–3018.
10. CLIFF, N. Dominance statistics: Ordinal analyses to answer ordinal questions. *Psychological bulletin* 114, 3 (1993), 494.
11. COHEN, R. A., CHOI, H., AND BAJIĆ, I. V. Lightweight compression of neural network feature tensors for collaborative intelligence. In *2020 IEEE International Conference on Multimedia and Expo (ICME)* (2020), IEEE, pp. 1–6.
12. CONOVER, W. J., AND IMAN, R. L. On multiple-comparisons procedures. *Los Alamos Sci. Lab. Tech. Rep. LA-7677-MS 1* (1979), 14.
13. CORDTS, M., OMRAN, M., RAMOS, S., REHFELD, T., ENZWEILER, M., BENENSON, R., FRANKE, U., ROTH, S., AND SCHIELE, B. The cityscapes dataset for semantic urban scene understanding. In *Proc. of the IEEE Conference on Computer Vision and Pattern Recognition (CVPR)* (2016).
14. DENG, S., ZHAO, H., FANG, W., YIN, J., DUSTNDAR, S., AND ZOMAYA, A. Y. Edge intelligence: The confluence of edge computing and artificial intelligence. *IEEE Internet of Things Journal* 7, 8 (2020), 7457–7469.
15. DIMOLITSAS, I., SPATHARAKIS, D., DECHOUMIOTIS, D., ZAFEIROPOULOS, A., AND PAPAVASSILIOU, S. Multi-application hierarchical autoscaling for kubernetes edge clusters. In *2023 IEEE International Conference on Smart Computing (SMARTCOMP)* (2023), IEEE, pp. 291–296.
16. DONG, C., HU, S., CHEN, X., AND WEN, W. Joint optimization with dnn partitioning and resource allocation in mobile edge computing. *IEEE Transactions on Network and Service Management* 18, 4 (2021), 3973–3986.
17. DUAN, Y., AND WU, J. Joint optimization of dnn partition and scheduling for mobile cloud computing. In *Proceedings of the 50th International Conference on Parallel Processing* (2021), pp. 1–10.
18. DWIVEDI, A. K., MALLAWAARACHCHI, I., AND ALVARADO, L. A. Analysis of small sample size studies using nonparametric bootstrap test with pooled resampling method. *Statistics in medicine* 36, 14 (2017), 2187–2205.
19. ELBAYAD, M., GU, J., GRAVE, E., AND AULI, M. Depth-adaptive transformer. *arXiv preprint arXiv:1910.10073* (2019).
20. ESHRATIFAR, A. E., ABRISHAMI, M. S., AND PEDRAM, M. Jointdnn: An efficient training and inference engine for intelligent mobile cloud computing services. *IEEE Transactions on Mobile Computing* 20, 2 (2019), 565–576.
21. ESHRATIFAR, A. E., ESMAILI, A., AND PEDRAM, M. Bottlenet: A deep learning architecture for intelligent mobile cloud computing services. In *2019 IEEE/ACM International Symposium on Low Power Electronics and Design (ISLPED)* (2019), IEEE, pp. 1–6.
22. FAN, A., STOCK, P., GRAHAM, B., GRAVE, E., GRIBONVAL, R., JEGOU, H., AND JOULIN, A. Training with quantization noise for extreme model compression. *arXiv preprint arXiv:2004.07320* (2020).
23. FANG, J., SHAFIEE, A., ABDEL-AZIZ, H., THORSLEY, D., GEORGIADIS, G., AND HASOUN, J. H. Post-training piecewise linear quantization for deep neural networks. In *Computer Vision–ECCV 2020: 16th European Conference, Glasgow, UK, August 23–28, 2020, Proceedings, Part II 16* (2020), Springer, pp. 69–86.
24. FIANDRINO, C., PIZARRO, A. B., MATEO, P. J., RAMIRO, C. A., LUDANT, N., AND WIDMER, J. openleon: An end-to-end emulation platform from the edge data center to the mobile user. *Computer Communications* 148 (2019), 17–26.
25. GARG, S., JAIN, A., LOU, J., AND NAHMIAS, M. Confounding tradeoffs for neural network quantization. *arXiv preprint arXiv:2102.06366* (2021).
26. GARG, S., LOU, J., JAIN, A., GUO, Z., SHASTRI, B. J., AND NAHMIAS, M. Dynamic precision analog computing for neural networks. *IEEE Journal of Selected Topics in Quantum Electronics* 29, 2: Optical Computing (2022), 1–12.
27. GHOLAMI, A., KIM, S., DONG, Z., YAO, Z., MAHONEY, M. W., AND KEUTZER, K. A survey of quantization methods for efficient neural network inference. In *Low-Power Computer Vision*. Chapman and Hall/CRC, 2022, pp. 291–326.
28. GOODFELLOW, I., Bengio, Y., AND COURVILLE, A. *Deep Learning*. MIT Press, 2016. <http://www.deeplearningbook.org>.
29. GÖRMEZ, A., DASARI, V. R., AND KOYUNCU, E. E 2 cm: Early exit via class means for efficient supervised and unsupervised learning. In *2022 International Joint Conference on Neural Networks (IJCNN)* (2022), IEEE, pp. 1–8.
30. GÖRMEZ, A., AND KOYUNCU, E. Class based thresholding in early exit semantic segmentation networks. *arXiv preprint arXiv:2210.15621* (2022).
31. GRAY, R. M., AND NEUHOFF, D. L. Quantization. *IEEE transactions on information theory* 44, 6 (1998), 2325–2383.
32. GREENGARD, S. Ai on edge. *Commun. ACM* 63, 9 (aug 2020), 18–20.
33. GUADAGNOLI, E., AND VELICER, W. F. Relation of sample size to the stability of component patterns. *Psychological bulletin* 103, 2 (1988), 265.
34. HAMPAU, R. M., KAPTEIN, M., VAN EMDEN, R., ROST, T., AND MALAVOLTA, I. An empirical study on the performance and energy consumption of ai containerization strategies for computer-vision tasks on the edge. In *Proceedings of the International Conference on Evaluation and Assessment in Software Engineering 2022* (2022), pp. 50–59.
35. HAWKS, B., DUARTE, J., FRASER, N. J., PAPPALARDO, A., TRAN, N., AND UMUROGLU, Y. Ps and qs: Quantization-aware pruning for efficient low latency neural network inference. *Frontiers in Artificial Intelligence* 4 (2021), 676564.
36. HE, X., AND CHENG, J. Learning compression from limited unlabeled data. In *Proceedings of the European Conference on Computer Vision (ECCV)* (2018), pp. 752–769.
37. HESS, M. R., AND KROMREY, J. D. Robust confidence intervals for effect sizes: A comparative study of cohen'sd and cliff's delta under non-normality and heterogeneous variances. In *annual meeting of the American Educational Research Association* (2004), vol. 1, Citeseer.
38. HOLM, S. A simple sequentially rejective multiple test procedure. *Scandinavian journal of statistics* (1979), 65–70.
39. HU, C., BAO, W., WANG, D., AND LIU, F. Dynamic adaptive dnn surgery for inference acceleration on the edge. In *IEEE INFOCOM 2019-IEEE Conference on Computer Communications* (2019), IEEE, pp. 1423–1431.

40. HU, D., AND KRISHNAMACHARI, B. Fast and accurate streaming cnn inference via communication compression on the edge. In *2020 IEEE/ACM Fifth International Conference on Internet-of-Things Design and Implementation (IoTDI)* (2020), IEEE, pp. 157–163.
41. HUBARA, I., NAHSHAN, Y., HANANI, Y., BANNER, R., AND SOUDRY, D. Improving post training neural quantization: Layer-wise calibration and integer programming. *arXiv preprint arXiv:2006.10518* (2020).
42. JANKOWSKI, M., GÜNDÜZ, D., AND MIKOŁAJCZYK, K. Joint device-edge inference over wireless links with pruning. In *2020 IEEE 21st international workshop on signal processing advances in wireless communications (SPAWC)* (2020), IEEE, pp. 1–5.
43. JEONG, H.-J., JEONG, I., LEE, H.-J., AND MOON, S.-M. Computation offloading for machine learning web apps in the edge server environment. In *2018 IEEE 38th International Conference on Distributed Computing Systems (ICDCS)* (2018), IEEE, pp. 1492–1499.
44. JIANG, Z. M., AND HASSAN, A. E. A survey on load testing of large-scale software systems. *IEEE Transactions on Software Engineering* 41, 11 (2015), 1091–1118.
45. KANG, Y., HAUSWALD, J., GAO, C., ROVINSKI, A., MUDGE, T., MARS, J., AND TANG, L. Neurosurgeon: Collaborative intelligence between the cloud and mobile edge. *ACM SIGARCH Computer Architecture News* 45, 1 (2017), 615–629.
46. KRISHNAMOORTHI, R. Quantizing deep convolutional networks for efficient inference: A whitepaper. *arXiv preprint arXiv:1806.08342* (2018).
47. KÜNAS, C. A. Optimizing machine learning models training in the cloud.
48. LASKARIDIS, S., VENIERIS, S. I., ALMEIDA, M., LEONTIADIS, I., AND LANE, N. D. Spinn: synergistic progressive inference of neural networks over device and cloud. In *Proceedings of the 26th annual international conference on mobile computing and networking* (2020), pp. 1–15.
49. LECUN, Y., BENGIO, Y., AND HINTON, G. Deep learning. *nature* 521, 7553 (2015), 436–444.
50. LEE, J. C., KIM, Y., MOON, S., AND KO, J. H. A splittable dnn-based object detector for edge-cloud collaborative real-time video inference. In *2021 17th IEEE International Conference on Advanced Video and Signal Based Surveillance (AVSS)* (2021), IEEE, pp. 1–8.
51. LEE, J. H., HA, S., CHOI, S., LEE, W.-J., AND LEE, S. Quantization for rapid deployment of deep neural networks. *arXiv preprint arXiv:1810.05488* (2018).
52. LI, E., ZHOU, Z., AND CHEN, X. Edge intelligence: On-demand deep learning model co-inference with device-edge synergy. In *Proceedings of the 2018 Workshop on Mobile Edge Communications* (2018), pp. 31–36.
53. LI, G., LIU, L., WANG, X., DONG, X., ZHAO, P., AND FENG, X. Auto-tuning neural network quantization framework for collaborative inference between the cloud and edge. In *Artificial Neural Networks and Machine Learning–ICANN 2018: 27th International Conference on Artificial Neural Networks, Rhodes, Greece, October 4–7, 2018, Proceedings, Part I* 27 (2018), Springer, pp. 402–411.
54. LI, H., ZHANG, H., QI, X., YANG, R., AND HUANG, G. Improved techniques for training adaptive deep networks. In *Proceedings of the IEEE/CVF international conference on computer vision* (2019), pp. 1891–1900.
55. Li, Y., GONG, R., TAN, X., YANG, Y., HU, P., ZHANG, Q., YU, F., WANG, W., AND GU, S. Brecq: Pushing the limit of post-training quantization by block reconstruction. *arXiv preprint arXiv:2102.05426* (2021).
56. LIANG, H., SANG, Q., HU, C., CHENG, D., ZHOU, X., WANG, D., BAO, W., AND WANG, Y. Dnn surgery: Accelerating dnn inference on the edge through layer partitioning. *IEEE Transactions on Cloud Computing* (2023).
57. LIN, T.-Y., MAIRE, M., BELONGIE, S., HAYS, J., PERONA, P., RAMANAN, D., DOLLÁR, P., AND ZITNICK, C. L. Microsoft coco: Common objects in context. In *Computer Vision–ECCV 2014: 13th European Conference, Zurich, Switzerland, September 6–12, 2014, Proceedings, Part V* 13 (2014), Springer, pp. 740–755.
58. LIU, D., KONG, H., LUO, X., LIU, W., AND SUBRAMANIAM, R. Bringing ai to edge: From deep learning’s perspective. *Neurocomputing* 485 (2022), 297–320.
59. LIU, W., ZHOU, P., ZHAO, Z., WANG, Z., DENG, H., AND JU, Q. Fastbert: a self-distilling bert with adaptive inference time. *arXiv preprint arXiv:2004.02178* (2020).
60. LO, C., SU, Y.-Y., LEE, C.-Y., AND CHANG, S.-C. A dynamic deep neural network design for efficient workload allocation in edge computing. In *2017 IEEE International Conference on Computer Design (ICCD)* (2017), IEEE, pp. 273–280.
61. LONG, J., SHELHAMER, E., AND DARRELL, T. Fully convolutional networks for semantic segmentation, 2015.
62. LU, D., AND WENG, Q. A survey of image classification methods and techniques for improving classification performance. *International journal of Remote sensing* 28, 5 (2007), 823–870.
63. LUO, D., YU, T., WU, Y., WU, H., WANG, T., AND ZHANG, W. Split: Qos-aware dnn inference on shared gpu via evenly-sized model splitting. In *Proceedings of the 52nd International Conference on Parallel Processing* (2023), pp. 605–614.
64. MATSUBARA, Y., BAIDYA, S., CALLEGARO, D., LEVORATO, M., AND SINGH, S. Distilled split deep neural networks for edge-assisted real-time systems. In *Proceedings of the 2019 Workshop on Hot Topics in Video Analytics and Intelligent Edges* (2019), pp. 21–26.
65. MATSUBARA, Y., CALLEGARO, D., SINGH, S., LEVORATO, M., AND RESTUCCIA, F. Bottleft: Learning compressed representations in deep neural networks for effective and efficient split computing. In *2022 IEEE 23rd International Symposium on a World of Wireless, Mobile and Multimedia Networks (WoWMoM)* (2022), IEEE, pp. 337–346.
66. MATSUBARA, Y., AND LEVORATO, M. Split computing for complex object detectors: Challenges and preliminary results. In *Proceedings of the 4th International Workshop on Embedded and Mobile Deep Learning* (2020), pp. 7–12.
67. MATSUBARA, Y., AND LEVORATO, M. Neural compression and filtering for edge-assisted real-time object detection in challenged networks. In *2020 25th International Conference on Pattern Recognition (ICPR)* (2021), IEEE, pp. 2272–2279.
68. MATSUBARA, Y., LEVORATO, M., AND RESTUCCIA, F. Split computing and early exiting for deep learning applications: Survey and research challenges. *ACM Computing Surveys* 55, 5 (2022), 1–30.
69. MATSUBARA, Y., YANG, R., LEVORATO, M., AND MANDT, S. Sc2 benchmark: Supervised compression for split computing. *arXiv e-prints* (2022), arXiv–2203.

70. MATSUBARA, Y., YANG, R., LEVORATO, M., AND MANDT, S. Supervised compression for resource-constrained edge computing systems. In *Proceedings of the IEEE/CVF Winter Conference on Applications of Computer Vision* (2022), pp. 2685–2695.
71. MELLER, E., FINKELSTEIN, A., ALMOG, U., AND GROBMAN, M. Same, same but different: Recovering neural network quantization error through weight factorization. In *International Conference on Machine Learning* (2019), PMLR, pp. 4486–4495.
72. MERKEL, D. Docker: Lightweight linux containers for consistent development and deployment. *Linux J.* 2014, 239 (mar 2014).
73. MINAEI, S., BOYKOV, Y., PORIKLI, F., PLAZA, A., KEHTARNAVAZ, N., AND TERZOPOULOS, D. Image segmentation using deep learning: A survey. *IEEE transactions on pattern analysis and machine intelligence* 44, 7 (2021), 3523–3542.
74. MOHAMMED, T., JOE-WONG, C., BABBAR, R., AND DI FRANCESCO, M. Distributed inference acceleration with adaptive dnn partitioning and offloading. In *IEEE INFOCOM 2020-IEEE Conference on Computer Communications* (2020), IEEE, pp. 854–863.
75. MURSHED, M. S., MURPHY, C., HOU, D., KHAN, N., ANANTHANARAYANAN, G., AND HUSSAIN, F. Machine learning at the network edge: A survey. *ACM Computing Surveys (CSUR)* 54, 8 (2021), 1–37.
76. NA, J., ZHANG, H., LIAN, J., AND ZHANG, B. Genetic algorithm-based online-partitioning branchynet for accelerating edge inference. *Sensors* 23, 3 (2023), 1500.
77. NAGEL, M., BAALEN, M. v., BLANKEVOORT, T., AND WELLING, M. Data-free quantization through weight equalization and bias correction. In *Proceedings of the IEEE/CVF International Conference on Computer Vision* (2019), pp. 1325–1334.
78. NAN, Y., JIANG, S., AND LI, M. Large-scale video analytics with cloud–edge collaborative continuous learning. *ACM Transactions on Sensor Networks* 20, 1 (2023), 1–23.
79. NESHATPOUR, K., HOMAYOUN, H., AND SASAN, A. Icnn: The iterative convolutional neural network. *ACM Transactions on Embedded Computing Systems (TECS)* 18, 6 (2019), 1–27.
80. OPENJA, M., NIKANJAM, A., YAHMED, A. H., KHOMH, F., MING, Z., ET AL. An empirical study of challenges in converting deep learning models. *arXiv preprint arXiv:2206.14322* (2022).
81. OSTERTAGOVA, E., OSTERTAG, O., AND KOVÁČ, J. Methodology and application of the kruskal-wallis test. In *Applied mechanics and materials* (2014), vol. 611, Trans Tech Publ, pp. 115–120.
82. PAGLIARI, D. J., CHIARO, R., MACII, E., AND PONCINO, M. Crime: Input-dependent collaborative inference for recurrent neural networks. *IEEE Transactions on Computers* 70, 10 (2020), 1626–1639.
83. PHUONG, M., AND LAMPERT, C. H. Distillation-based training for multi-exit architectures. In *Proceedings of the IEEE/CVF international conference on computer vision* (2019), pp. 1355–1364.
84. POMPONI, J., SCARDAPANE, S., AND UNCINI, A. A probabilistic re-intepretation of confidence scores in multi-exit models. *Entropy* 24, 1 (2021), 1.
85. PORTABALES, A. R., AND NORES, M. L. Dockemu: Extension of a scalable network simulation framework based on docker and ns3 to cover iot scenarios. In *SIMULTECH* (2018), pp. 175–182.
86. PORTABALES, A. R., AND NORES, M. L. Dockemu: An iot simulation framework based on linux containers and the ns-3 network simulator—application to coap iot scenarios. In *Simulation and Modeling Methodologies, Technologies and Applications: 8th International Conference, SIMULTECH 2018, Porto, Portugal, July 29-31, 2018, Revised Selected Papers* (2020), Springer, pp. 54–82.
87. QIAN, J., LI, J., MA, R., LIN, L., AND GUAN, H. Lg-ram: Load-aware global resource affinity management for virtualized multicore systems. *Journal of Systems Architecture* 98 (2019), 114–125.
88. RUSSAKOVSKY, O., DENG, J., SU, H., KRAUSE, J., SATHEESH, S., MA, S., HUANG, Z., KARPATHY, A., KHOSLA, A., BERNSTEIN, M., BERG, A. C., AND FEI-FEI, L. ImageNet Large Scale Visual Recognition Challenge. *International Journal of Computer Vision (IJCV)* 115, 3 (2015), 211–252.
89. SAKR, C., DAI, S., VENKATESAN, R., ZIMMER, B., DALLY, W., AND KHAILANY, B. Optimal clipping and magnitude-aware differentiation for improved quantization-aware training. In *International Conference on Machine Learning* (2022), PMLR, pp. 19123–19138.
90. SBAI, M., SAPUTRA, M. R. U., TRIGONI, N., AND MARKHAM, A. Cut, distil and encode (cde): Split cloud-edge deep inference. In *2021 18th Annual IEEE International Conference on Sensing, Communication, and Networking (SECON)* (2021), IEEE, pp. 1–9.
91. SCARDAPANE, S., SCARPINITI, M., BACCARELLI, E., AND UNCINI, A. Why should we add early exits to neural networks? *Cognitive Computation* 12, 5 (2020), 954–966.
92. SHAO, J., AND ZHANG, J. Bottlenet++: An end-to-end approach for feature compression in device-edge co-inference systems. In *2020 IEEE International Conference on Communications Workshops (ICC Workshops)* (2020), IEEE, pp. 1–6.
93. SHEN, M., LIANG, F., GONG, R., LI, Y., LI, C., LIN, C., YU, F., YAN, J., AND OUYANG, W. Once quantization-aware training: High performance extremely low-bit architecture search. In *Proceedings of the IEEE/CVF International Conference on Computer Vision* (2021), pp. 5340–5349.
94. SHOMRON, G., GABBAY, F., KURZUM, S., AND WEISER, U. Post-training sparsity-aware quantization. *Advances in Neural Information Processing Systems* 34 (2021), 17737–17748.
95. SOLDAINI, L., AND MOSCHITTI, A. The cascade transformer: an application for efficient answer sentence selection. *arXiv preprint arXiv:2005.02534* (2020).
96. SURYAVANSH, S., BOTHRA, C., CHIANG, M., PENG, C., AND BAGCHI, S. Tango of edge and cloud execution for reliability. In *Proceedings of the 4th Workshop on Middleware for Edge Clouds & Cloudlets* (2019), pp. 10–15.
97. TABANI, H., BALASUBRAMANIAM, A., ARANI, E., AND ZONOZOZ, B. Challenges and obstacles towards deploying deep learning models on mobile devices. *CoRR abs/2105.02613* (2021).
98. TAILOR, S. A., FERNANDEZ-MARQUES, J., AND LANE, N. D. Degree-quant: Quantization-aware training for graph neural networks. *arXiv preprint arXiv:2008.05000* (2020).

99. TEERAPITTAYANON, S., McDANEL, B., AND KUNG, H.-T. Branchynet: Fast inference via early exiting from deep neural networks. In *2016 23rd international conference on pattern recognition (ICPR)* (2016), IEEE, pp. 2464–2469.
100. TEERAPITTAYANON, S., McDANEL, B., AND KUNG, H.-T. Distributed deep neural networks over the cloud, the edge and end devices. In *2017 IEEE 37th international conference on distributed computing systems (ICDCS)* (2017), IEEE, pp. 328–339.
101. WANG, M., MO, J., LIN, J., WANG, Z., AND DU, L. Dynexit: A dynamic early-exit strategy for deep residual networks. In *2019 IEEE International Workshop on Signal Processing Systems (SiPS)* (2019), IEEE, pp. 178–183.
102. WANG, P., CHEN, P., YUAN, Y., LIU, D., HUANG, Z., HOU, X., AND COTTRELL, G. Understanding convolution for semantic segmentation, 2018.
103. WANG, X., HAN, Y., LEUNG, V. C., NIYATO, D., YAN, X., AND CHEN, X. Convergence of edge computing and deep learning: A comprehensive survey. *IEEE Communications Surveys & Tutorials* 22, 2 (2020), 869–904.
104. WANG, Y., SHEN, J., HU, T.-K., XU, P., NGUYEN, T., BARANIUK, R., WANG, Z., AND LIN, Y. Dual dynamic inference: Enabling more efficient, adaptive, and controllable deep inference. *IEEE Journal of Selected Topics in Signal Processing* 14, 4 (2020), 623–633.
105. WOHLIN, C., RUNESON, P., HÖST, M., OHLSSON, M. C., REGNELL, B., AND WESSLÉN, A. *Experimentation in software engineering*. Springer Science & Business Media, 2012.
106. WOŁCZYK, M., WÓJCIK, B., BALAZY, K., PODOLAK, I. T., TABOR, J., ŚMIEJA, M., AND TRZCINSKI, T. Zero time waste: Recycling predictions in early exit neural networks. *Advances in Neural Information Processing Systems* 34 (2021), 2516–2528.
107. WU, H., JUDD, P., ZHANG, X., ISAEV, M., AND MICIKEVICIUS, P. Integer quantization for deep learning inference: Principles and empirical evaluation. *arXiv preprint arXiv:2004.09602* (2020).
108. XIE, S., GIRSHICK, R., DOLLÁR, P., TU, Z., AND HE, K. Aggregated residual transformations for deep neural networks, 2017.
109. XIN, J., NOGUEIRA, R., YU, Y., AND LIN, J. Early exiting bert for efficient document ranking. In *Proceedings of SustaiNLP: Workshop on Simple and Efficient Natural Language Processing* (2020), pp. 83–88.
110. XIN, J., TANG, R., LEE, J., YU, Y., AND LIN, J. Deebert: Dynamic early exiting for accelerating bert inference. *arXiv preprint arXiv:2004.12993* (2020).
111. XING, Q., XU, M., LI, T., AND GUAN, Z. Early exit or not: Resource-efficient blind quality enhancement for compressed images. In *European Conference on Computer Vision* (2020), Springer, pp. 275–292.
112. YANG, L., HAN, Y., CHEN, X., SONG, S., DAI, J., AND HUANG, G. Resolution adaptive networks for efficient inference. In *Proceedings of the IEEE/CVF conference on computer vision and pattern recognition* (2020), pp. 2369–2378.
113. YANG, X., CHEN, D., QI, Q., WANG, J., SUN, H., LIAO, J., AND GUO, S. Adaptive dnn surgery for selfish inference acceleration with on-demand edge resource. *arXiv preprint arXiv:2306.12185* (2023).
114. YAO, S., LI, J., LIU, D., WANG, T., LIU, S., SHAO, H., AND ABDELZAHER, T. Deep compressive offloading: Speeding up neural network inference by trading edge computation for network latency. In *Proceedings of the 18th conference on embedded networked sensor systems* (2020), pp. 476–488.
115. ZAGORUYKO, S., AND KOMODAKIS, N. Wide residual networks, 2017.
116. ZENG, L., LI, E., ZHOU, Z., AND CHEN, X. Boomerang: On-demand cooperative deep neural network inference for edge intelligence on the industrial internet of things. *IEEE Network* 33, 5 (2019), 96–103.
117. ZHANG, L. L., HAN, S., WEI, J., ZHENG, N., CAO, T., YANG, Y., AND LIU, Y. Nn-meter: Towards accurate latency prediction of deep-learning model inference on diverse edge devices. In *Proceedings of the 19th Annual International Conference on Mobile Systems, Applications, and Services* (2021), pp. 81–93.
118. ZHANG, X., MOUNESAN, M., AND DEBROY, S. Effect-dnn: Energy-efficient edge framework for real-time dnn inference. In *2023 IEEE 24th International Symposium on a World of Wireless, Mobile and Multimedia Networks (WoWMoM)* (2023), IEEE, pp. 10–20.
119. ZHAO, R., HU, Y., DOTZEL, J., DE SA, C., AND ZHANG, Z. Improving neural network quantization without retraining using outlier channel splitting. In *International conference on machine learning* (2019), PMLR, pp. 7543–7552.
120. ZHOU, L., WEN, H., TEODORESCU, R., AND DU, D. H. Distributing deep neural networks with containerized partitions at the edge. In *2nd USENIX Workshop on Hot Topics in Edge Computing (HotEdge 19)* (2019).
121. ZHOU, W., XU, C., GE, T., McAULEY, J., XU, K., AND WEI, F. Bert loses patience: Fast and robust inference with early exit. *Advances in Neural Information Processing Systems* 33 (2020), 18330–18341.
122. ZHOU, Z., CHEN, X., LI, E., ZENG, L., LUO, K., AND ZHANG, J. Edge intelligence: Paving the last mile of artificial intelligence with edge computing. *Proceedings of the IEEE* 107, 8 (2019), 1738–1762.

## Appendices

### Appendix A Graphical Illustrations of Manual Operators

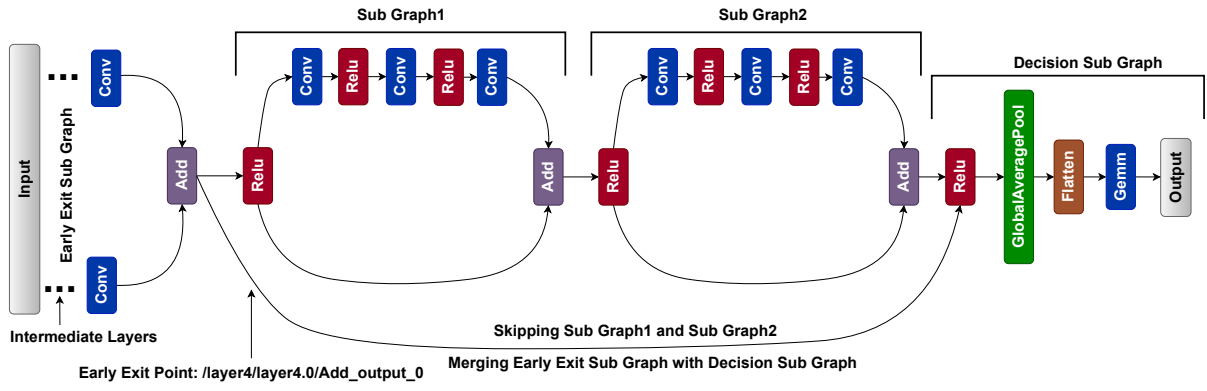


Fig. 8: Graphical Illustration of Early Exiting for ResNet and ResNext

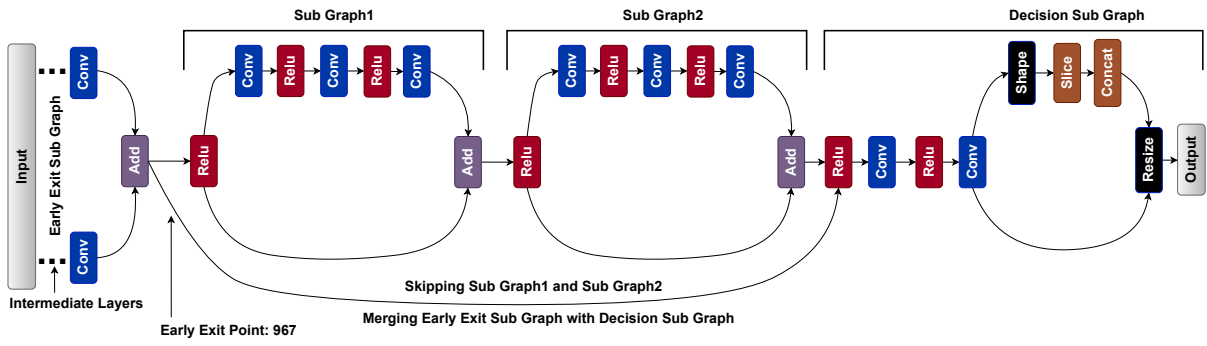


Fig. 9: Graphical Illustration of Early Exiting for FCN

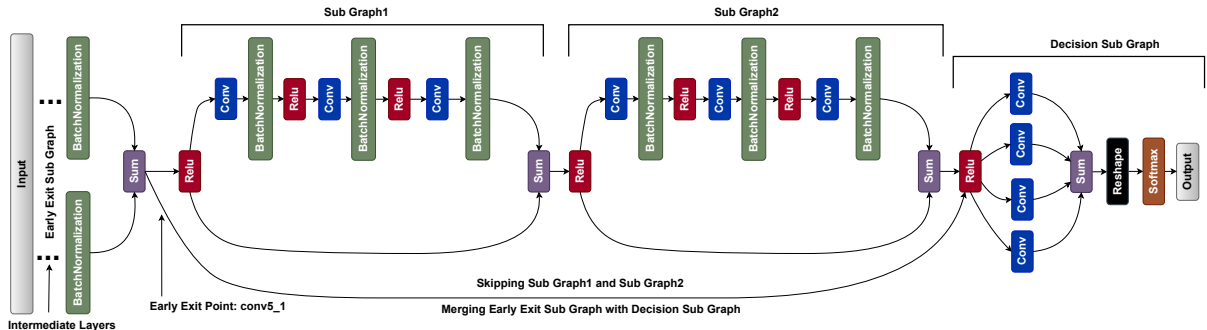


Fig. 10: Graphical Illustration of Early Exiting for DUC

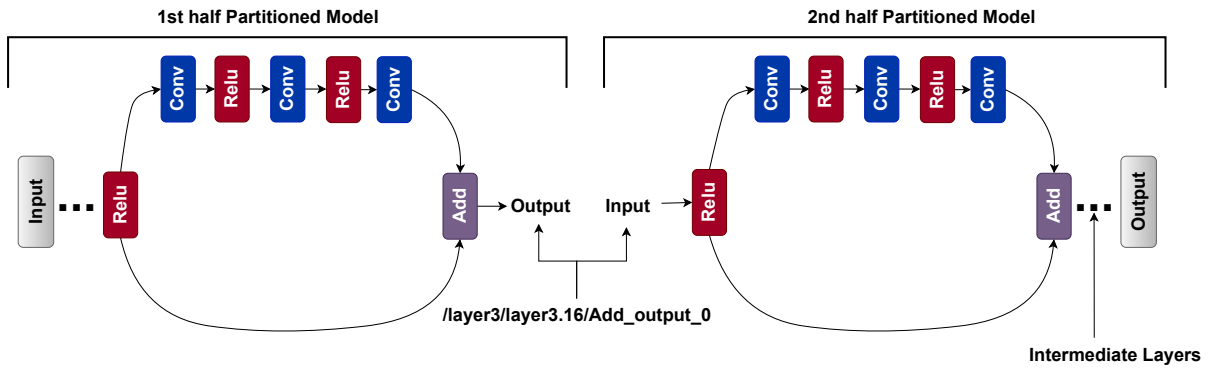


Fig. 11: Graphical Illustration of Model Partitioning for ResNet and ResNext

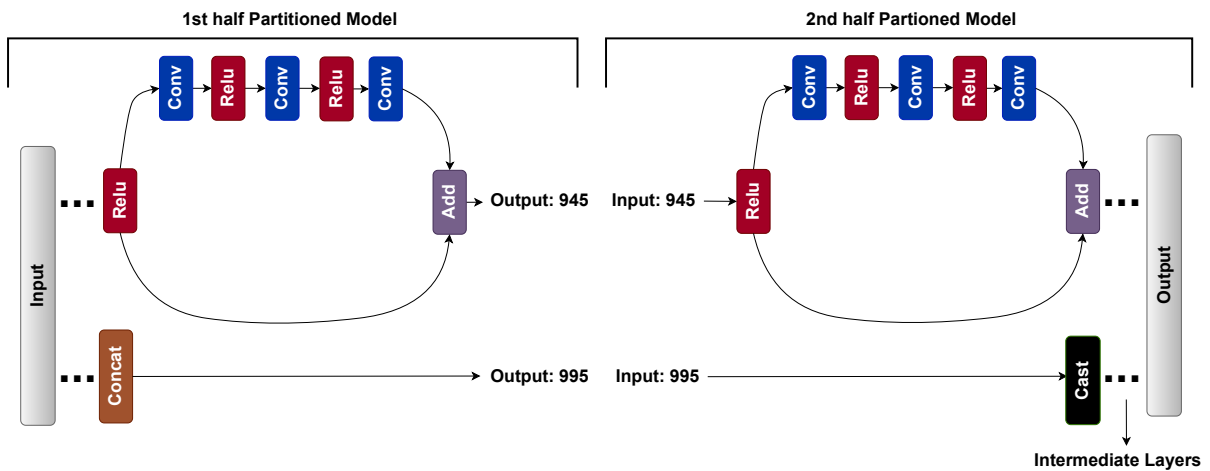


Fig. 12: Graphical Illustration of Model Partitioning for FCN

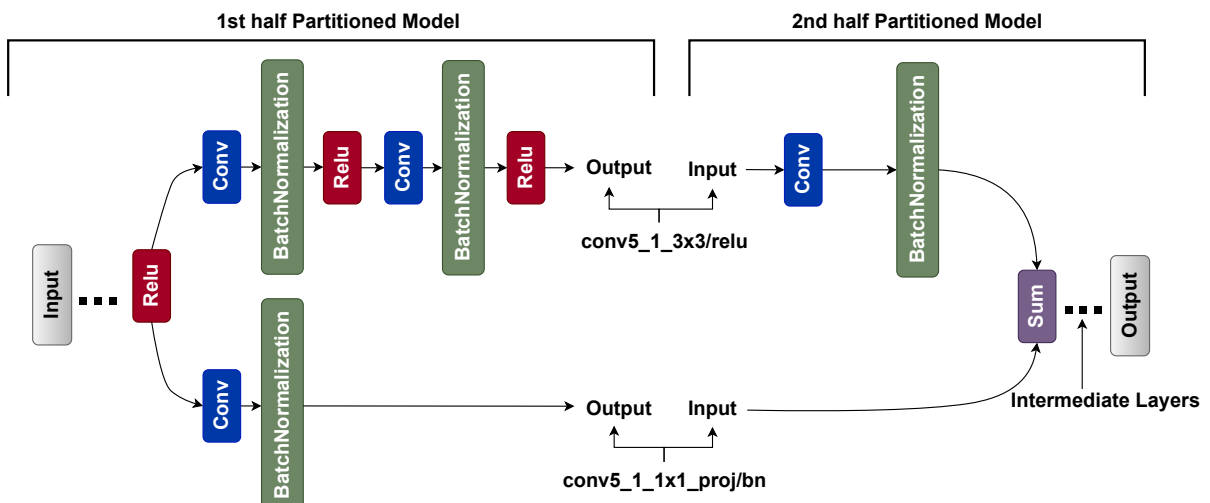


Fig. 13: Graphical Illustration of Model Partitioning for DUC

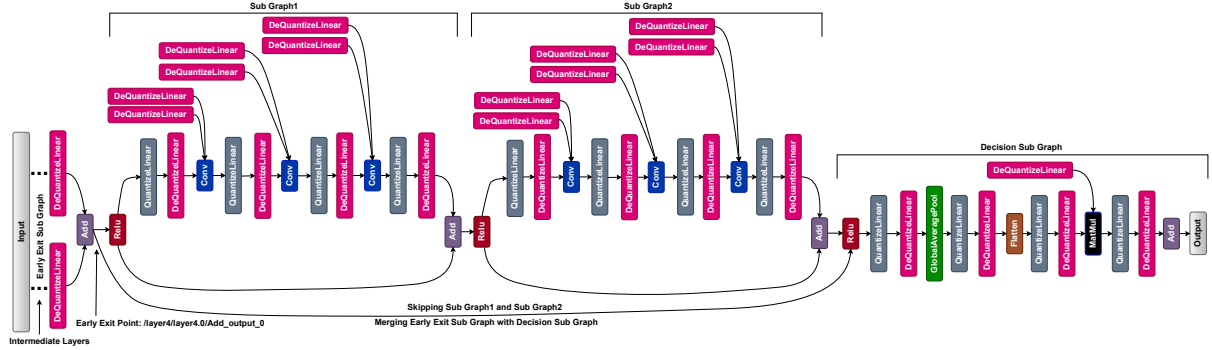


Fig. 14: Graphical Illustration of Quantized Early Exit for ResNet and ResNext

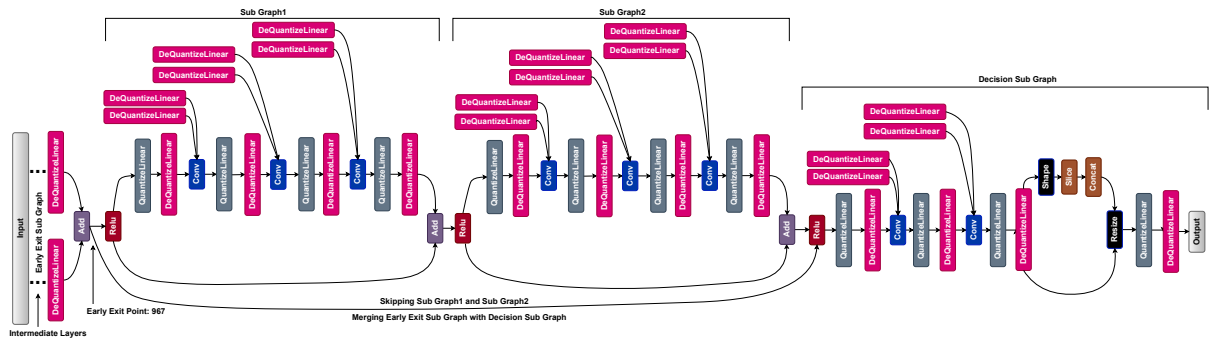


Fig. 15: Graphical Illustration of Quantized Early Exit for FCN

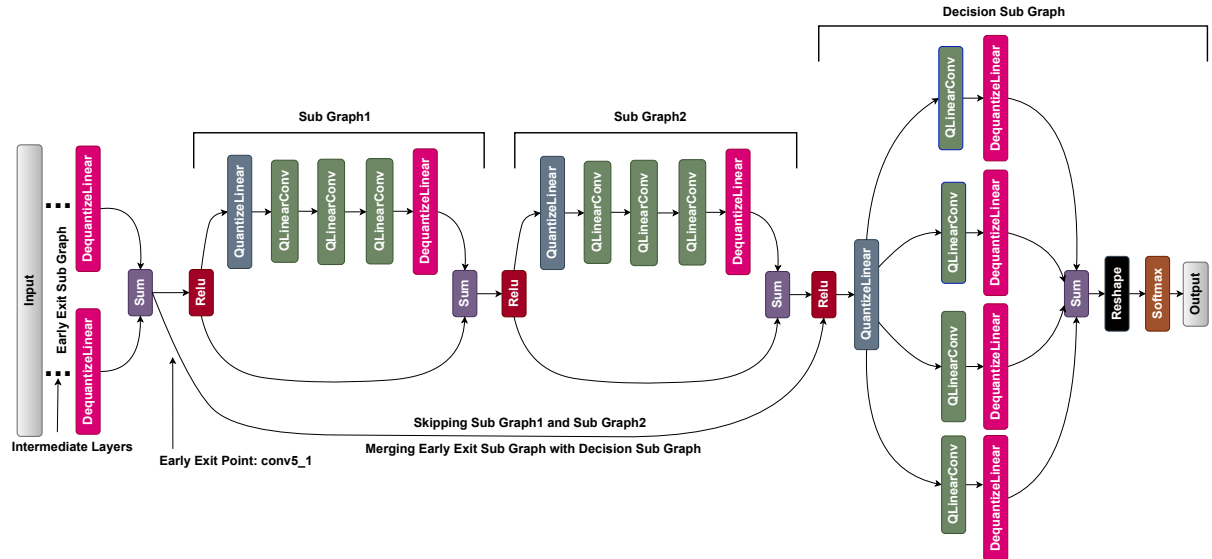


Fig. 16: Graphical Illustration of Quantized Early Exit for DUC

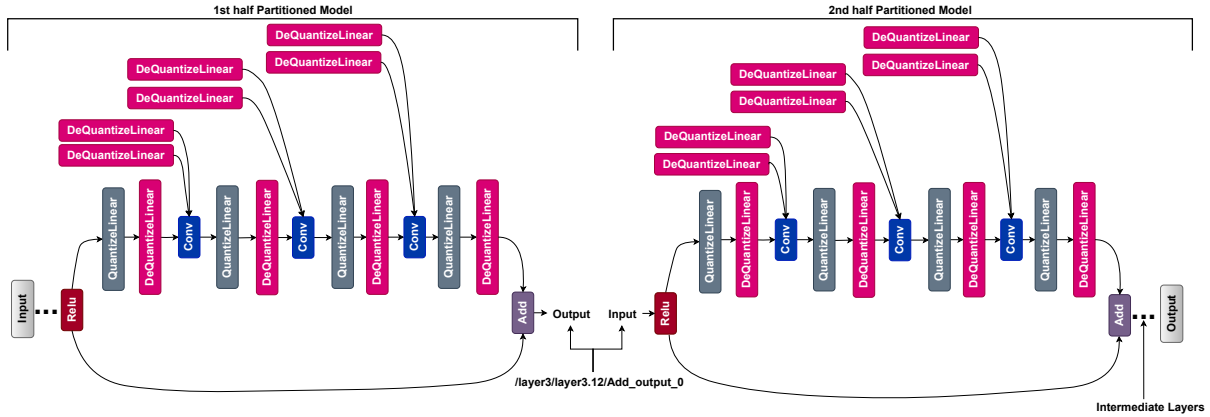


Fig. 17: Graphical Illustration of Quantized Early Exit Partitioning for ResNet and ResNext

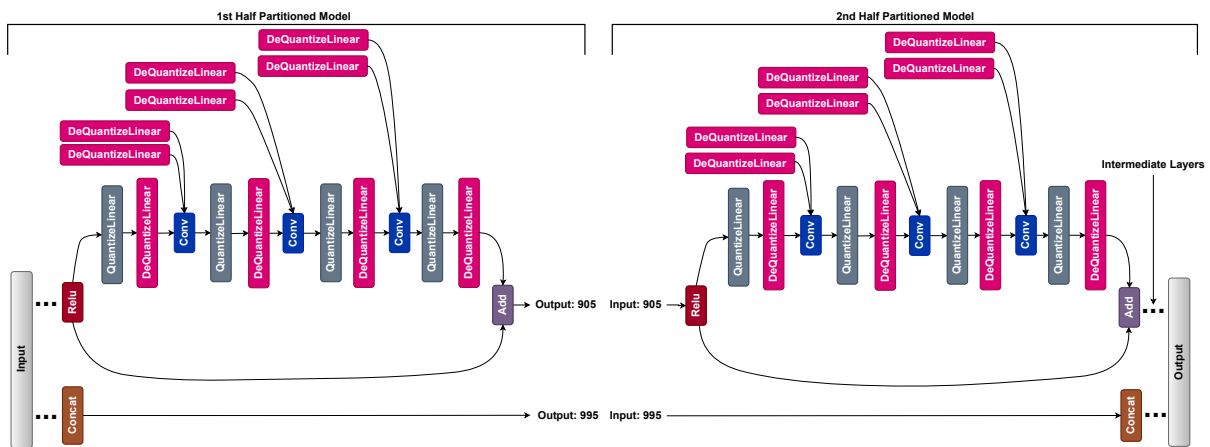


Fig. 18: Graphical Illustration of Quantized Early Exit Partitioning for FCN

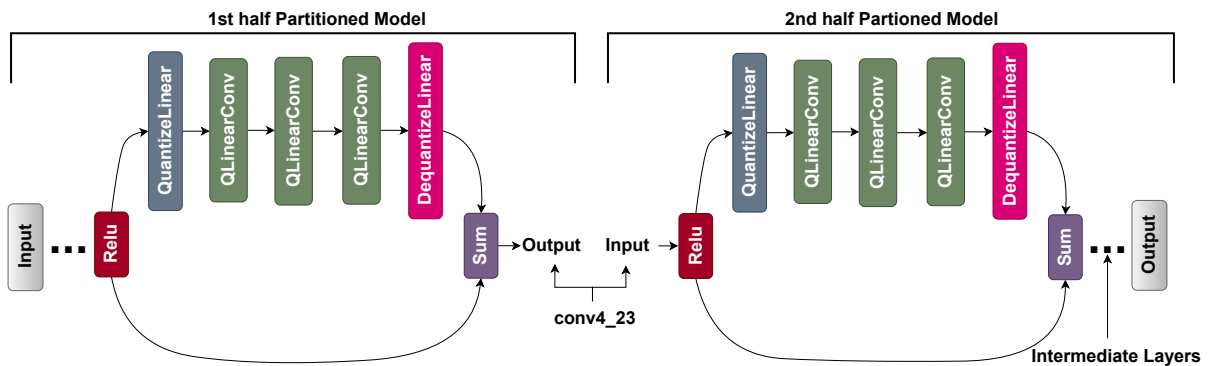


Fig. 19: Graphical Illustration of Quantized Early Exit Partitioning for DUC